

Tectonics and sedimentation of the Lower and Middle Pleistocene mixed siliciclastic/bioclastic sedimentary successions of the Ionian Peloritani Mts (NE Sicily, Southern Italy): the onset of opening of the Messina Strait

Research Article

Agata Di Stefano^{1*}, Sergio G. Longhitano^{2†}

1 Department of Geological Science, University of Catania, 95129, Catania, Italy

2 Department of Geological Science, University of Basilicata, 85100, Potenza, Italy

Received 14 November 2008; accepted 30 January 2009

Abstract: Biostratigraphic analyses carried out on siliciclastic/bioclastic deposits discontinuously cropping out along the Ionian flank of NE Sicily, indicate that they form two sedimentary events of Early and Middle Pleistocene, respectively. Vertical facies successions, showing transgressive trends, suggest that sedimentation occurred within semi-enclosed marine embayments, where sublittoral coastal wedges developed on steep ramp-type shelves. Sediments accumulated in shoreface to offshore transitions along steep bottom profiles. This depositional scenario was strongly conditioned by the tectonic activity of the rift zone linking Western Calabria and Eastern Sicily. The effects of glacio-eustatism were also recognized. According to our reconstruction, the study area was controlled by a transfer fault system which affected the coastal margin producing major episodes of uplift and subsidence. Block-faulting was responsible for significant cannibalization and recycling of older deposits during the Middle Pleistocene. Such a tectonic setting can be considered the precursor scenario for the formation of the Messina Strait between Calabria and Sicily. This narrow, linear basin influences the hydrodynamic setting of sublittoral deposits along the Ionian coast of Sicily, giving rise to strong flood/ebb tidal currents. The uppermost part of the Middle Pleistocene succession recognized in the study area is indeed dominated by tide-influenced associations of sedimentary structures which most likely record the first stage of the opening of this 'seaway' of the central Mediterranean Sea.

Keywords: NE Sicily • Messina Strait • Early-Middle Pleistocene • facies analysis and biostratigraphy • tectonics and sedimentation

© Versita Warsaw

1. Introduction

Plio-Pleistocene cool-water biocalcarenitic-dominated sediments, forming isolated or clustered coastal wedges, represent one of the most common types of deposits crop-

*E-mail: distefan@unict.it

†E-mail: sergio.longhitano@unibas.it

ping out along the northeastern coast of Sicily (Southern Italy) [1–9]. These deposits are mainly formed by mixed siliciclastic and bioclastic fractions derived from the local bedrock units and skeletal fragments.

Along the Mediterranean coasts, these sediments intermittently developed during the Plio-Pleistocene and have been described in recent literature in the context of various depositional settings. Some of these settings show evidence of syndepositional tectonics [10–24].

Depositional systems often show well-developed clinoform geometry prograding away from the coast and forming shore-parallel linear bodies. The basin margins from which the wedges developed were affected in some cases by persistent tectonic movements, which controlled the geometric stacking of the clinoforms [25] or inhibited the formation of clinoforms because of the steep gradient of the coastal bottom profile [26]. Active tectonics affecting a coastal margin frequently produce a composite coastal morphology, forming alternating small gulfs, embayments and promontories. Generally, this coastal setting allowed the sedimentation of adjacent shore prisms, separated by small promontories and characterized by different depositional and sedimentary features.

In such settings sedimentation is strongly controlled by tectonics that may produce incomplete depositional cycles of several hierarchical orders, and bounding surfaces defining abrupt facies transitions and depth conditions. Glacioeustatic signal can be identified in lower-rank sequences or parasequences [27].

Recent studies e.g.: [22] have pointed out that in NE Sicily (along the southern margin of the Tyrrhenian Basin) Plio-Pleistocene sediments consist of tectonically-controlled, transgressive successions of shallow-marine to deeper marine neritic environments. Three main depositional sequences (R1, R2 and R3) ranging in age from Middle Pliocene to Middle Pleistocene can be recognized.

In this work we present the results of detailed facies analysis and nannofossil biostratigraphic study, carried out on the Lower-Middle Pleistocene sedimentary succession cropping out along the Ionian side of NE Sicily (Peloritani Mts). Here, the sedimentary succession is mainly characterized by mixed, siliciclastic/bioclastic sediments ('mixed' sandstones [28] or 'hybrid arenites' [29]) forming isolated coastal wedges. In these deposits the bioclastic fraction is represented by foramol-assemblages (sensu [30] and [31]). During the Plio-Pleistocene time interval, initial WNW-ESE and later NE-SW, normal fault systems broke this segment of the Ionian coast into several sectors [32–34]. This caused the formation of uplifted promontories separated by small bays, and favored the development of laterally-varying sedimentary conditions. Our study demonstrates that sedimentation occurred diachronously

across the Ionian margin and that it was progressively more influenced by tide dominated bi-directional tractional currents towards the Middle Pleistocene. This change in current regime was most likely related to opening of the Messina Strait.

2. Tectonic and stratigraphic setting of NE Sicily (Peloritani Mts)

Calabria and NE Sicily represent a segment of the Neogene Apennine-Maghrebide orogenic belt (Calabrian Arc, [35]; Figure 1, inset), which developed in the central Mediterranean Sea as a result of collision between Africa and Europe [36–39], and northwesterly subduction and roll-back of the Adriatic-Ionian slab [34, 40–43].

NE Sicily presently separates the Tyrrhenian basin (to the NW) and the Ionian basin (to the SE) (Figure 1, inset), both representing back-arc areas [34]. The Neogene deposits cropping out in this part of Sicily (Peloritani Mts in Figure 1), record the tectonic and sedimentary evolution of this complex area during the opening of the southern Tyrrhenian basin and of the eastern Ionian basin. From the Late Oligocene onward, the terrigenous sedimentary successions of the Peloritani Mts (Figure 2A) formed distinct depositional cycles bounded by regional unconformities, each of them indicating a stage in the complex polyphase evolution of the area ([44–46] and references therein).

Late Oligocene to Early Miocene sediments are associated with a compressional regime, during which a series of perched forearc basins formed, separated by intervening highs of crystalline basement [45]. From the Middle Miocene, the Tyrrhenian margin of the northern Sicilian sector (Figure 1, inset) was affected by the extensional tectonic phase preceding the opening of the Tyrrhenian Basin. Thick clastic successions accumulated in down-thrown areas (San Pier Niceto Fm). During the same period up to the Early Pliocene, collisional processes still dominated the Ionian margin of the eastern Sicilian sector (Figure 1, inset). From the Late Pliocene onward, the Ionian sector was also affected by extensional faulting, which fragmented the orogen into structural highs and subsiding local basins [45].

The resultant Plio-Pleistocene sediments [10, 22, 33, 47, 48] are arranged into several unconformity-bounded stratigraphic units, ranging from Early Pliocene (Trubi Fm) up to late Middle Pleistocene (Messina Gravels and Sands Fm [33, 49]).

The Messina Strait is a narrow, linear basin located between Calabria and Sicily [50]. This basin formed in the Late Pliocene due to normal faulting in a belt extending

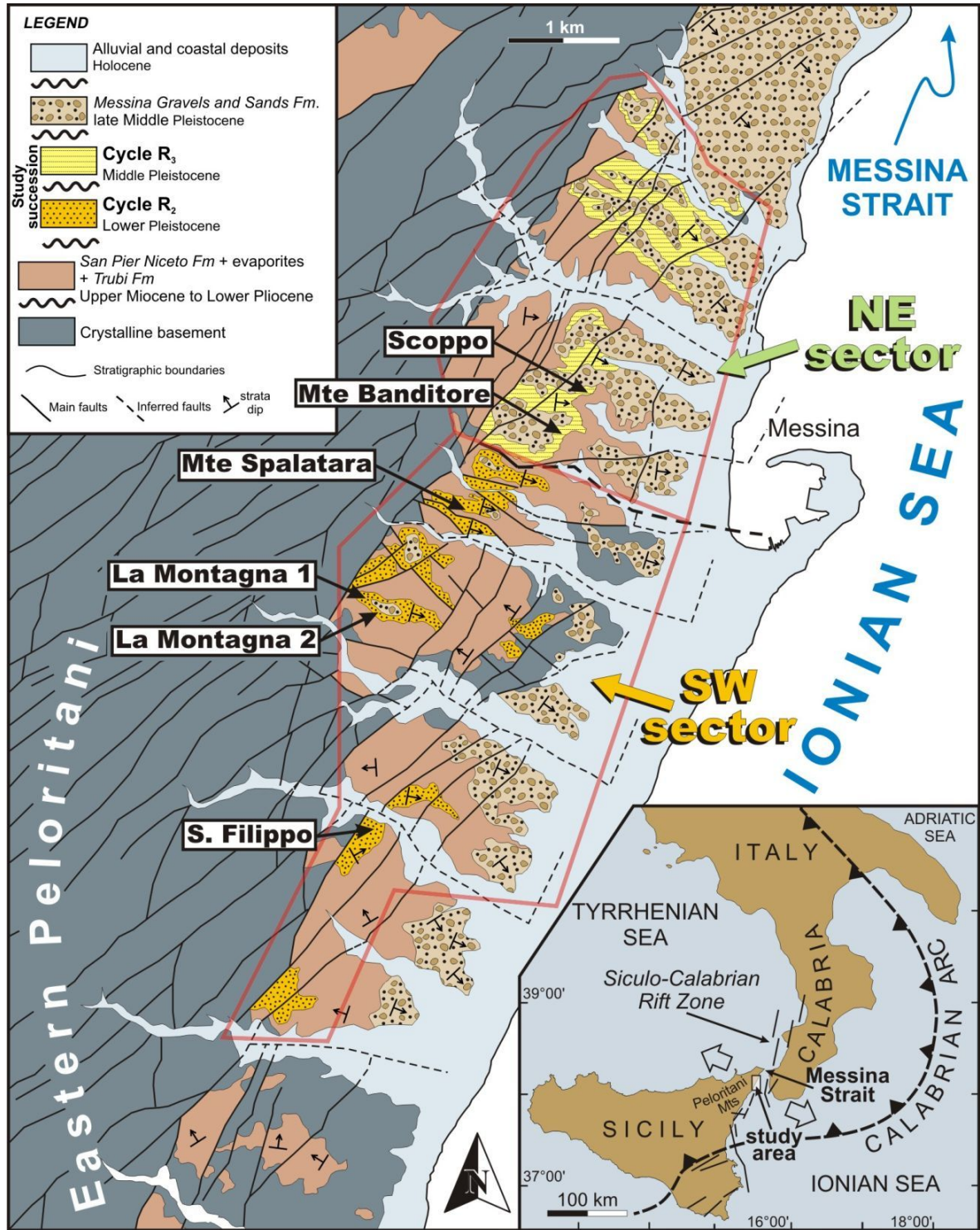


Figure 1. Simplified geological map of the study area (modified after [33]) and regional location in the central Mediterranean Sea (inset; arrows indicate the main extensional direction of the “Siculo-Calabrian Rift Zone” [54]). Cycles R2 and R3 are confined within two sectors SW and NE, respectively. Locations of the stratigraphic logs are indicated. The pre-Pleistocene sedimentary units (Middle-Upper Miocene San Pier Niceto Fm, Messinian evaporites and Lower Pliocene Trubi Fm) have been grouped to better highlight the Pleistocene successions. The internal red line bounding the two sectors may be likely considered as an approximation of the coastlines during the sedimentation of cycles R2 and R3.

from western Calabria to southern Sicily ([45, 46, 51, 52] and references therein). This NE-SW-oriented fault system, associated with destructive historical earthquakes, is known in the literature as the “Siculo-Calabrian Rift Zone” ([34, 53, 54]; Figure 1, inset) and is characterized by minor, approximately orthogonal faults, which control the present-day setting of the Sicilian Ionian coast [39, 46, 55–59]. Most of the minor faults associated with this system show vertical displacements of the sedimentary successions and volcanic products (from Mt. Etna) together with fault escarpments that suggest short-term vertical slip-rates of 1–2 mm/year [53, 60]. From the Early–Middle Pleistocene, Calabria and north-eastern Sicily were affected by strong uplift, which progressively decreased toward the north and the west [61–66]. This uplift was caused by displacement along extensional faults that controlled local domains of subsidence, including the Messina Strait [46, 52, 53, 59, 61, 67, 68].

The Messina Strait is presently characterized by sea-floor erosion, which is responsible for the irregular bottom topography and scarcity of sediment cover. Where sediment accumulation is present, strong currents flowing along the axis of the strait [69, 70] generate coarse-grained sand-waves that migrate from north to south and vice versa. Currents, ranging in velocity from 1 to 3 m/s [71], are generated by amplification of out-of-phase tidal cycles that occur every six hours [70].

The sedimentary succession examined in this study (cycles R2 and R3 in Figure 1 and Figure 2B) represents part of the Plio–Pleistocene deposits characterizing the emerged Calabrian (to the north) and Sicilian (to the south) margins of the present Messina Strait (eastern Peloritani Mts) (Figure 1). These deposits overlie remnants of the Early Pliocene Trubi Formation or lie directly on the older substratum. They are unconformably overlain by the Messina Gravel and Sand Formation (Figure 2B).

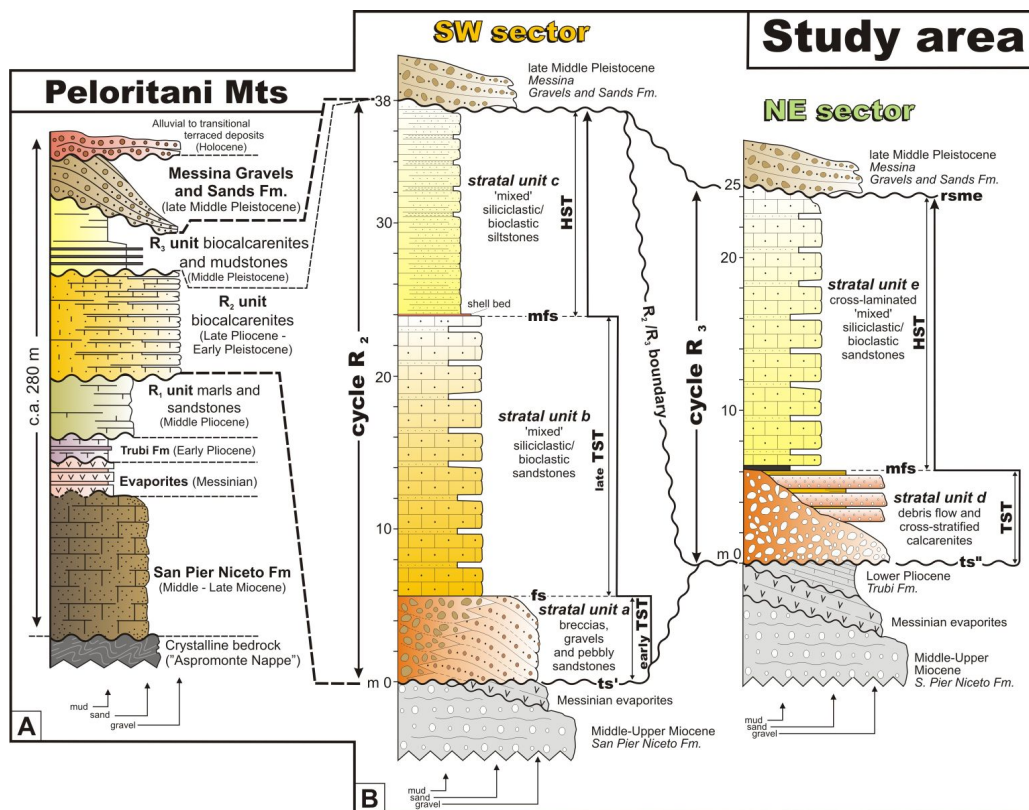


Figure 2. (A) General stratigraphy of Neogene sedimentary succession of the Peloritani Mts. (B) Lower-Middle Pleistocene interval cropping out in the study area. The succession has been subdivided into two cycles R2 and R3. Letter symbols: ts = transgressive surface; fs = flooding surface; mfs = maximum flooding surface; rsme = regressive surface of marine erosion; TST = transgressive systems tract; HST = highstand systems tract.

3. Methods

The study is based primarily on field observations. Most stratigraphic data were gathered from sections exposed in a number of natural and artificial outcrops exhibiting a range of exposure conditions and orientations. A number of small digs and scarps along roads provided additional information. Facies analysis was carried out on

6 vertical sections spaced 100-600 m apart (total thickness 129.2 m) and combined with interpretation of photomosaics. Grain sizes, sedimentary structures, trace and body fossils, palaeoflow indicators and stratigraphic surfaces were identified. The main bounding surfaces were traced physically from section to section and used as key-elements for stratigraphic correlation.

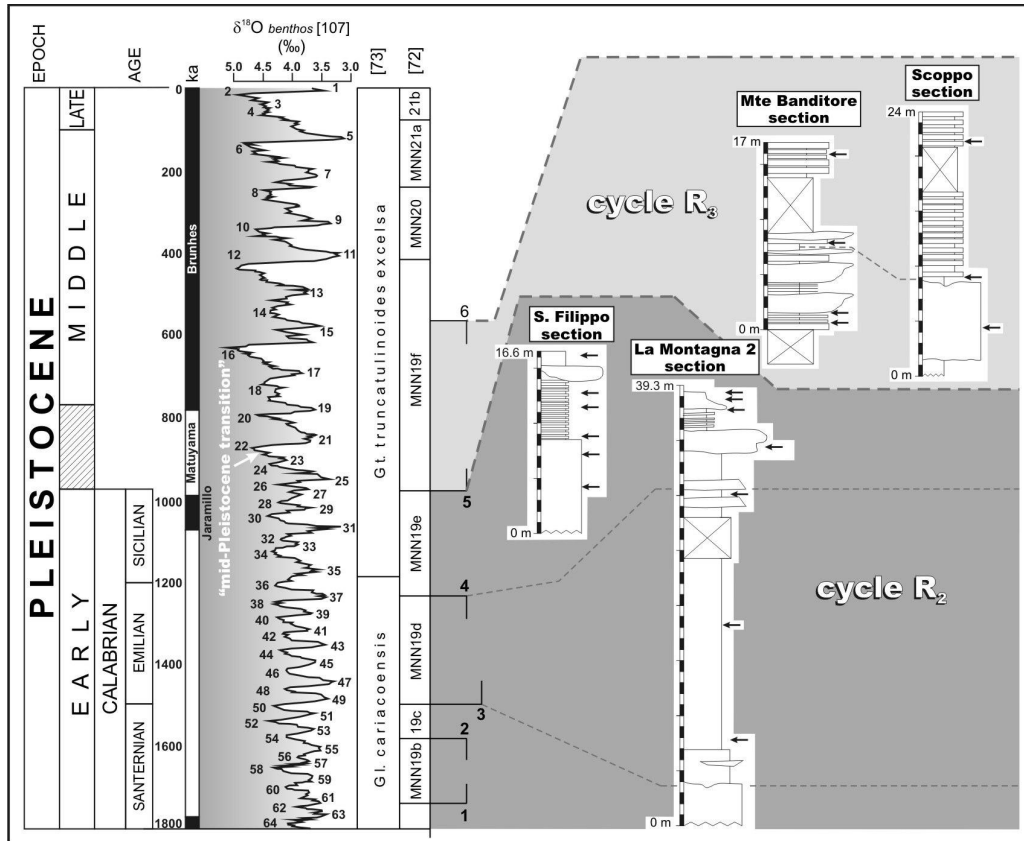


Figure 3. Bio- and chrono-stratigraphic correlations of the studied sections based on calcareous nannofossil analyses. Black arrows indicate the position of the analyzed samples. Numbers indicate the nannofossil bioevents: 1 = First Occurrence of *Gephyrocapsa oceanica* s.l.; 2 = Last Occurrence of *Calcidiscus macintyre*; 3 = First Occurrence of *Gephyrocapsa* "large"; 4 = Last Occurrence of *Gephyrocapsa* "large"; 5 = First Occurrence of *Gephyrocapsa* sp.3; 6 = Last Occurrence of *Gephyrocapsa* sp.3. Due to lacking of a formal GSSP (Global Stratotype Section and Point), the Early/Middle Pleistocene boundary corresponds to the interval between the First Occurrence of *Gephyrocapsa* sp.3 (0.99 M.a.) and the base of the Brunhes chron (0.78 Ma, dashed interval of the second left column).

Approximately 20 rock samples were found suitable for the calcareous nannofossil study. These samples were prepared following the standard methodology for smear-slides [72] and references therein, and then analyzed with a light microscope at a magnification of x1000-1250. The biostratigraphic scheme proposed by [73] for the Mediter-

ranean region was adopted for the present study and compared with the foraminiferal scheme of [74], amended by [75] (Figure 3). According to the most recent literature [76-78], the Early/Middle Pleistocene boundary is located in the interval between the base of biozone MNN19f (dated at 0.99 Ma [75]), and the Brunhes/Matuyama mag-

netic reversal (0.78 Ma [78]).

The studied sedimentary successions can be considered fining-upward cycles [79] or transgressive T cycles [80], because they show vertical facies trends that suggest sedimentation during relative sea-level rises.

4. Stratigraphy and sedimentology of the Lower-Middle Pleistocene succession of the Ionian Peloritani Mts

The Lower-Middle Pleistocene strata considered in the present study crop out along the Ionian side of the Peloritani Mts (NE Sicily), between the elevations of 160 m and 270 m above sea level (a.s.l.) due to a long-term uplift of the area [53, 60]. These sediments form several isolated outcrops very similar to each other in their stratigraphic and sedimentological characteristics, and for this reason they were considered as an unique isochronous succession by previous authors [10, 33, 47, 48].

According to our data, these sediments were subdivided into two main units which, on the basis of their general stratigraphic trends and biostratigraphic constraints (Table 1 and Figure 3), can be considered as 'cycles' [79]. These cycles are chiefly equivalent to those recently documented for the northern sector of the Peloritani Mts (Tyrrhenian coast of Sicily) [22]. For this reason, the same coding nomenclature R2 and R3 (from the name 'Rometta' of outcrop locality, Tyrrhenian coast of NE Sicily) to identify the two cycles has been adopted (Figure 2). No Middle-Upper Pliocene sediments (depositional sequence R1 in the Tyrrhenian sector [22]) occur in the examined outcrops.

In the Ionian sector, cycles R2 and R3 are physically separated and crop out in two main coastal areas, located to the SW and NE respectively (Figure 1). The lowermost cycle R2 occurs in the SW sector. It is composed of three main strata units, cropping out between the localities of San Filippo, La Montagna (Figures 5, 7A and 7B) and Monte Spalatara.

Table 1. List of calcareous nannofossils identified in selected samples from the Lower and Middle Pleistocene cycles R2 and R3 cropping out along the Ionian sector of NE Sicily and biostratigraphic and chronological attributions.

Cycles	Calcareous Nannofossil	Biozone [73]	Time interval	Age
R3	<i>Calcidiscus leptoporus</i>			
	<i>Coccolithus pelagicus</i>	MNN19f	distribution range of	MIDDLE PLEISTOCENE
	<i>Dictyococcites</i> spp.		<i>Gephyrocapsa</i> sp.3	
	<i>Helicosphaera carteri</i>		0.99-0.58 My [75]	
	<i>Gephyrocapsa oceanica</i> s.l. [73]			
	<i>Gephyrocapsa</i> "small" [73]			
	<i>Gephyrocapsa</i> sp.3 [73]			
	<i>Pseudoemiliania lacunosa</i>			
	<i>Reticulofenestra</i> spp.			
	UPPER PART			
R2	<i>Calcidiscus leptoporus</i>			
	<i>Coccolithus pelagicus</i>	MNN19e	1.25-0.99 My [75]	EARLY PLEISTOCENE (SICILIAN)
	<i>Dictyococcites</i> spp.			
	<i>Gephyrocapsa</i> "small" [73]			
	<i>Helicosphaera carteri</i>			
	<i>H. sellii</i>			
	<i>Pseudoemiliania lacunosa</i>			
	<i>Reticulofenestra</i> spp.			
		LOWER PART		
	<i>Calcidiscus leptoporus</i>			EARLY PLEISTOCENE (EMILIAN)
	<i>Coccolithus pelagicus</i>			
	<i>Dictyococcites</i> spp.	MNN19d	1.5-1.25 My [75]	
<i>Helicosphaera carteri</i>				
<i>H. sellii</i>				
<i>Pseudoemiliania lacunosa</i>				
<i>Gephyrocapsa</i> "small" [73]				
<i>Gephyrocapsa oceanica</i> s.l. [73]				
<i>Gephyrocapsa</i> "large" [73]				
	<i>Reticulofenestra</i> spp.			

Age	Cycles	Stratal Units	Facies Association	Facies codification, lithology and main sedimentary structures	Fossil association	Depositional processes and environments		
Middle Pleistocene	R ₃	HST	e	-	<i>Facies cbc - Cross-laminated biocalcarenites</i> Regular alternance of cross-laminated biocalcarenitic thin layers and siltstones. The palaeocurrents show opposite direction of palaeoflows suggesting the tidal influence.	Fragments of indistinct molluscs and corals in fine bioclasts.	Lower shoreface to offshore transition sedimentation mainly influenced by tidal ebb/flood tidal currents (Messina Strait).	
		mfS						
		TST	d	sc	<i>Facies Df - Chaotic Debris Flow deposit</i> Very thick chaotic deposit of debris flow sediments made of recycled bedrock- and R ₂ -deriving clasts. <i>Facies Smb - Siltstones and microbreccia</i> Laminated siltstones alternated to coarser tabular strata of fine breccia. <i>Facies Dd - Debris flow deposits</i> Organised, often reverse-graded, coarse-grained tabular beds.	Fragments of indistinct molluscs and corals in fine bioclasts.	Emplaced of scarp-derived debris falls and flows; Uni-directional offshore-directed tractive current alternated to organised bioclastic turbidites; Cohesionless debris flow deposits emplaced along the base ramp slope.	
	ts ^{II}							
	Early Pleistocene (Emilian - Sicilian)	R ₂	HST	c	-	<i>Facies bs - Bioclastic siltstones</i> Monotonous repetition of thin beds of siltstones intensely bioturbated with rare and indistinct plain-parallel lamination. Rare lenticular beds of fine bioclastic calcarenites occur.	Brachiopods, molluscs, echinoderms and corals.	Fall-out accumulation of bioclastic fines in open marine setting. Rare storm wavy episodes suggests offshore transition environments.
			mfS		shell bed			
TST			b	bc	<i>Facies bss - Bioclastic sandstones and siltstones</i> Monotonous alternation of 10-20 cm thick tabular beds, made of bioclastic sandstones and siltstones, characterized by pervasive planar- and cross-lamination. <i>Facies ic - Intraformational channelfills</i> Infill of channelised, concave up beds, made of intraformational calcareous and granitic + metamorphic large clasts.	Brachiopods and subordinate bivalves, echinoderms, bryozoans, cirripeds, serpulids and foraminifers. Highly fragmented fossils.	Uni-directional storm-induced downwelling and offshore-directed currents influencing sediments (<i>bbs</i>) along a lower shoreface along a middle to outer ramp; Incised chute and/or gullies filled by intraclasts (<i>ic</i>) along the ramp slope.	
deepening								
late								
early								
ts ^I								

Figure 4. Summary of the sedimentary facies, fossil associations and inferred depositional processes and environments reconstructed within the stratal units comprising the study succession. The two cycles (R₂ and R₃) show both deepening vertical trends in their facies assemblages and record two transgressive stages of Early and Middle Pleistocene, respectively. The R₂/R₃ superimposition is only for graphic reason. We remind that the two cycles crop out in separate geographic sectors without any physical overlap.

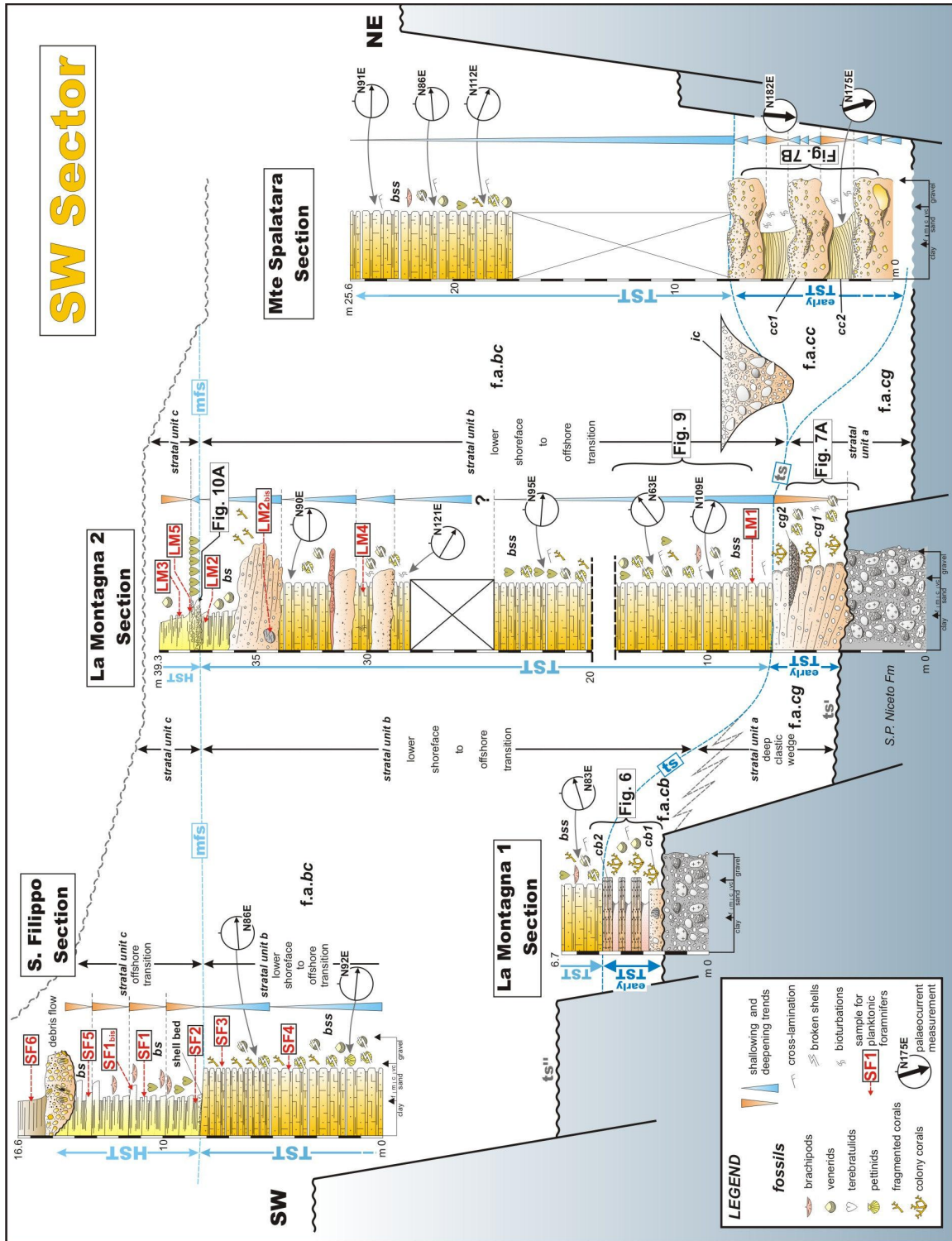


Figure 5. Sedimentological logs, including sequence stratigraphy interpretations, from the coastal ramp-type shelf of cycle R2 shown in Figure 2. The sections of San Filippo, La Montagna (1 and 2) and Monte Spalatarà are SW-NE-oriented and show the main facies associations comprising the sedimentary succession in the SW sector of the study area. Letter symbols: ts (I and II) = transgressive surfaces; mfs = maximum flooding surface; TST = transgressive systems tract; HST= highstand systems tract. In the scheme, outcrop photographs are reported in their correspondent stratigraphic intervals.

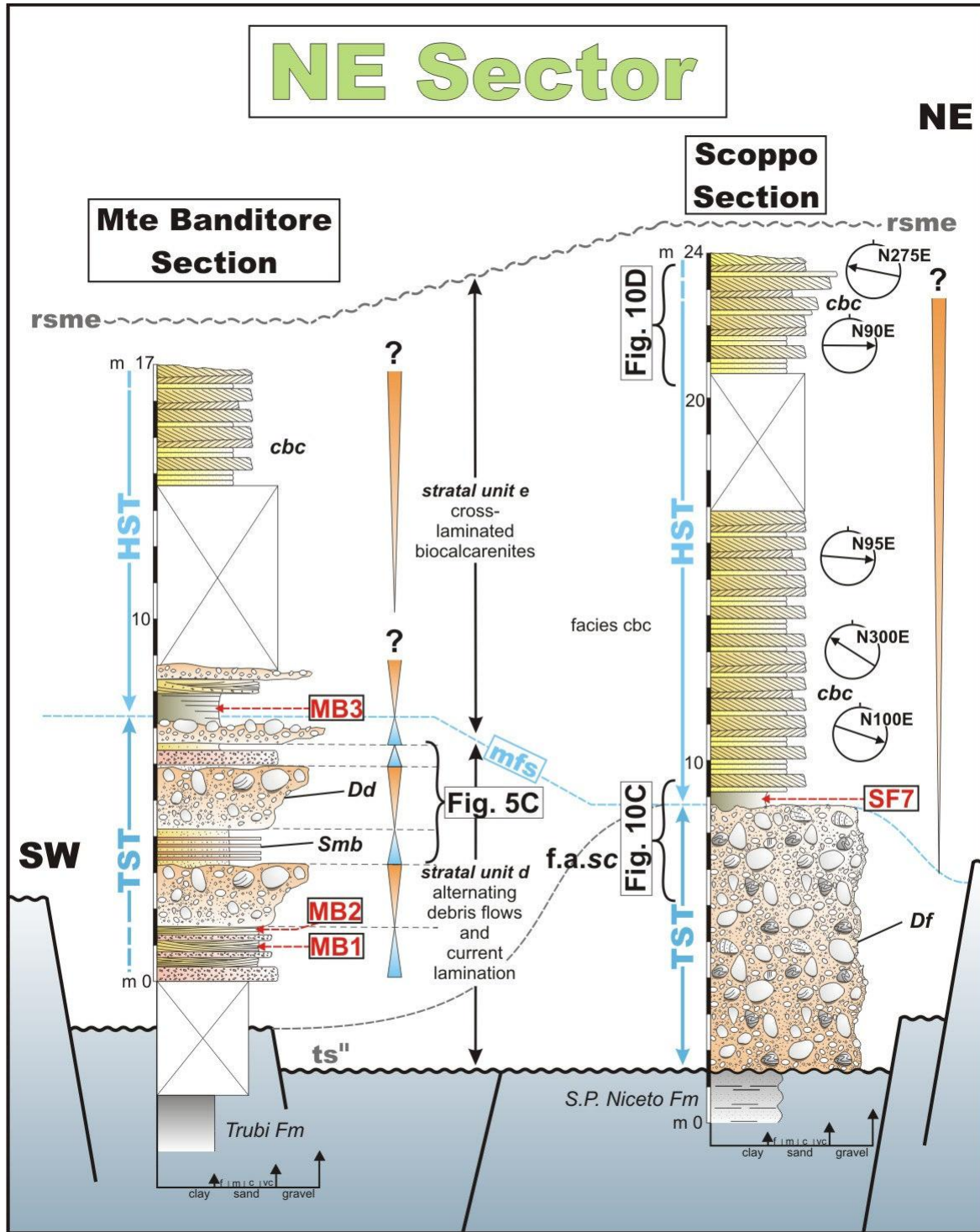


Figure 6. Sedimentological logs of Monte Banditore and Scoppo sections, corresponding to the sedimentary succession of cycle R3 exposed in the NE sector of the studied area. For legend explanation, see Figure 5. Letter symbols: ts (I and II) = transgressive surfaces; mfs = maximum flooding surface; rsme = regressive surface of marine erosion; TST = transgressive systems tract; HST = highstand systems tract. In the scheme, outcrop photographs are reported in their correspondent stratigraphic intervals.

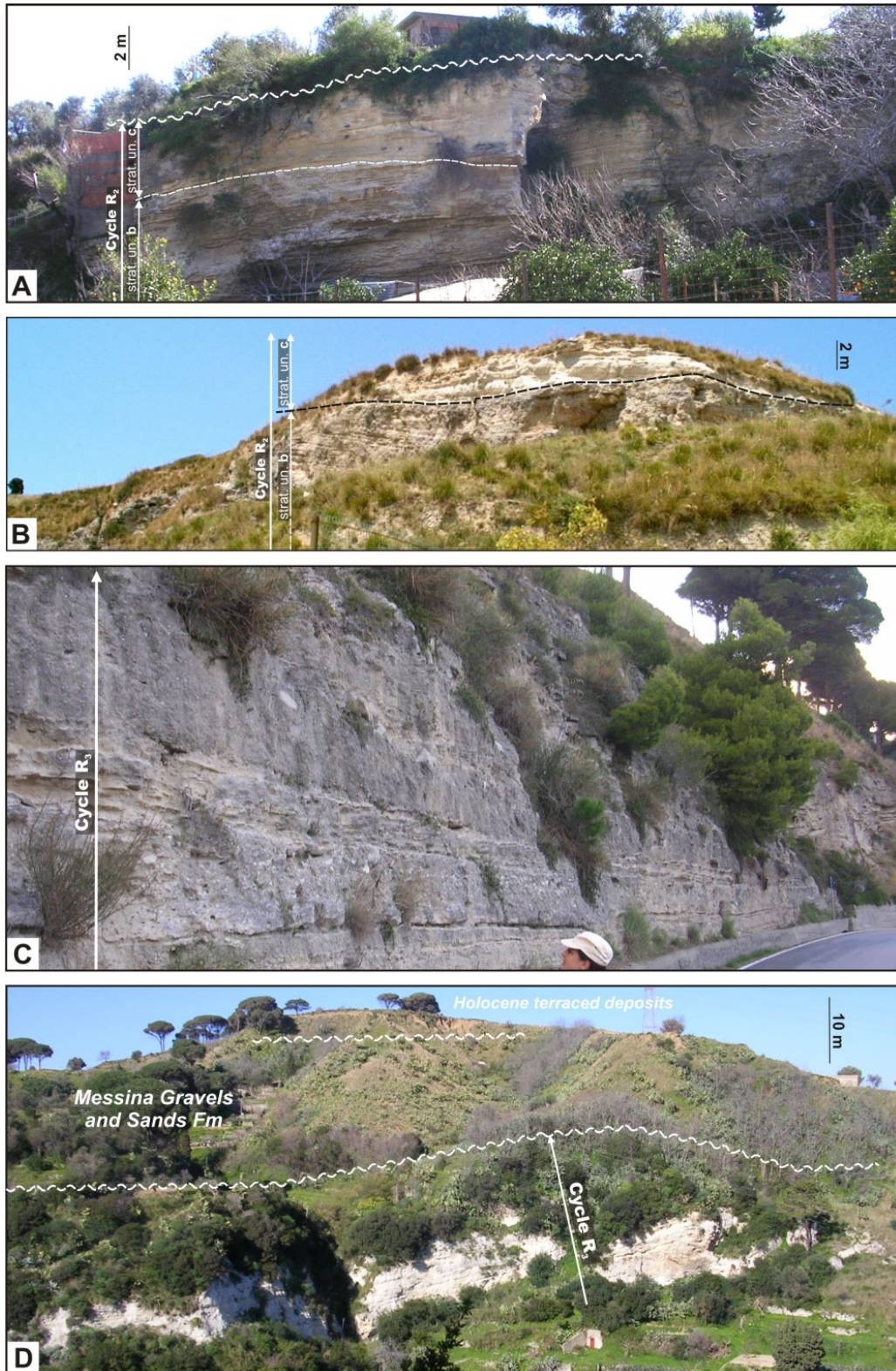


Figure 7. Major outcrops of the study area. (A) San Filippo and (B) La Montagna sections showing cycle R2. Both the photographs illustrate the vertical sharp transition (dotted line) from Stratal unit *b* to Stratal unit *c*, interpreted as TST and HST, respectively. (C) Alternating inverse graded strata of chaotic large clasts and laminated beds (facies association *sc*) along the Monte Banditore section, pertaining to the TST of cycle R3. (D) Topmost part of cycle R3 near the Scoppo section. The upper surface (undulate line) represents a regressive surface of marine erosion, marked by the progradation of the overlying Messina Gravels and Sands Fm.

In contrast, the NE sector is occupied by the younger cycle R3, that never lies upon the cycle R2 deposits. In this area, two different stratal units can be recognized between Monte Banditore and Scoppo (Figures 6, 7C and 7D). Both the SW and the NE sectors are dominated by bioclastic packstones and grainstones to fine-grained rudstones. Only the lowermost units contain a significant terrigenous fraction.

4.1. Cycle R2

In the Tyrrhenian sector of the Peloritani Mts, cycle R2 is a complete depositional sequence spanning the Late Pliocene to Early Pleistocene [22]. In contrast, in the Ionian sector (present study) the correlative succession starts from the Early Pleistocene Emilian substage (Figure 3). In fact, the nannofossil content is characterized in the lower part by the presence of *Gephyrocapsa* “large” (sensu [73]) which defines the MNN19d biozone (Emilian in age), and by dominant *Gephyrocapsa* “small” in the uppermost part, identifying the Early Pleistocene (Sicilian) MNN19e biozone. The time interval ranges from 1.5 Ma (base of MNN19d biozone, [75]) to 0.99 Ma (top of MNN19e biozone [75]; see Table 1 for a complete nannofossil list). The overall geometry displays a gradual wedging-out updip, and a relatively rapid lensing out at the distal termination, where the succession is overlain by terrigenous Holocene-to-Present coastal sediments (Figure 1). The outcrops extend a few hundred meters along the SSW-NNE-oriented palaeo-shoreline. The succession is subhorizontal to gently seaward-dipping and presents some facies variability and thickness differences. The general stratigraphic trend shows an apparent upward fining and deepening represented by vertical changes from bioturbated bioclastic packstone to fine bioclastic grainstone. The depositional cycle R2 can be subdivided into three stratal units (*a*, *b* and *c* in Figure 4).

4.1.1. Stratal unit *a*

Stratal unit *a* crops out at the base of La Montagna hill and erosively overlies the Middle-Upper Miocene San Pier Niceto Formation and the Messinian evaporites. The contact is marked by an angular unconformity (surface *ts*¹ in Figure 5). Stratal unit *a* forms a seaward-thickening wedge and shows a complex system of facies assemblages that have been subdivided, from proximal to distal, into three facies associations *pb*, *cg* and *cc* (Figure 4; La Montagna 1, La Montagna 2 and Monte Spalatara sections in Figure 5).

Facies association *pb* forms the inner edge of a wedge-shaped unit cropping out at the base of La Montagna 1 section. This facies association is represented by facies

pb1 and *pb2*. Facies *pb1* is a few meters thick polygenic breccias, composed of angular calcareous, arenitic, granitic and metamorphic gravels. Sediments are organized into massive, indistinctly-bedded strata lapping against cliffed and intensely bored metamorphic bedrock. The matrix is represented by mainly bioclastic sands and granules (Figure 8A). Basinwards, facies *pb1* laterally passes to facies *pb2* represented by pebbly calcirudites organized into indistinct 0.4–0.8 m thick, seawards-dipping strata. These deposits are poorly sorted and the primary bedding is often interrupted by the occurrence of coral colonies (Figures 8B and 8C). The matrix is composed of unsorted gravel-sized bioclasts, granules and sand. Strata alternate with fine-grained, bioclastic-rich sandy layers, including brachiopods with articulated valves (Figures 8D and 8E). The coral content is dominated by the presence of *Lophelia pertusa*, *Madrepora oculata* and *Desmophyllum cristagalli* and subordinate *Enallopsammia scil-lae* and *Dendrophyllia cornigera* [81].

Facies association *pb* evolves basinwards to facies association *cg*, subdivided into facies *cg1* and *cg2* (Figure 4). Facies *cg1* consists of matrix-supported clinostatified pebbly sandstones (La Montagna 2 section in Figure 5), organized into an ESE-thickening sigmoidal unit. This unit progrades on the Upper Miocene substrate and is bounded at the top by a flat surface (Figure 9A). The clasts, similar in composition to those observed within facies *pb*, show a higher degree of roundness and are organized into clinostatified beds dipping at 10°–12° basinwards. Foreset strata are formed by normal-graded mixed terrigenous granules and large bioclasts. Facies *cg2* is mainly represented by metamorphic, well-rounded pebbles and granules organized into lenticular layers, 0.5–1.2 m wide and 0.2–0.3 m thick. These layers form small erosive channel-fills encased within the deposits of facies *cg1*.

At the base of Monte Spalatara, Stratal unit *a* is represented by facies association *cc* (Figure 5). It consists of two alternating facies: facies *cc1* is represented by siliciclastic gravels and massive sands with scattered pebbles organized into 1.4–2.3 m thick beds. These beds form multiple, often amalgamated channel-fill deposits, each 30–40 cm thick (3–5 lenses per bed), and are characterized by normal grading and indistinct lenticular concave-up geometries with erosive bases. These beds also rhythmically alternate with the sediments of facies *cc2* (Figure 9B). Facies *cc2* consists of fine bioclastic/siliciclastic sands, characterized by angular to tangential cross-stratification forming 1–1.5 m thick subaqueous dunes (Figure 9C). The internal architecture of these dunes consists of repeated bundles of coarsening- and fining-upwards bed-sets 12–27 cm thick (*n/s* in Figure 10) interrupted by diffused bio-

turbation, and showing palaeocurrent directions measured in the cross-laminated strata ranging from N140° E to N 180° E. The base of the dunes is an irregular undulated

surface, whilst the top is often erosive with diffused loading and flame structures (Figure 10).

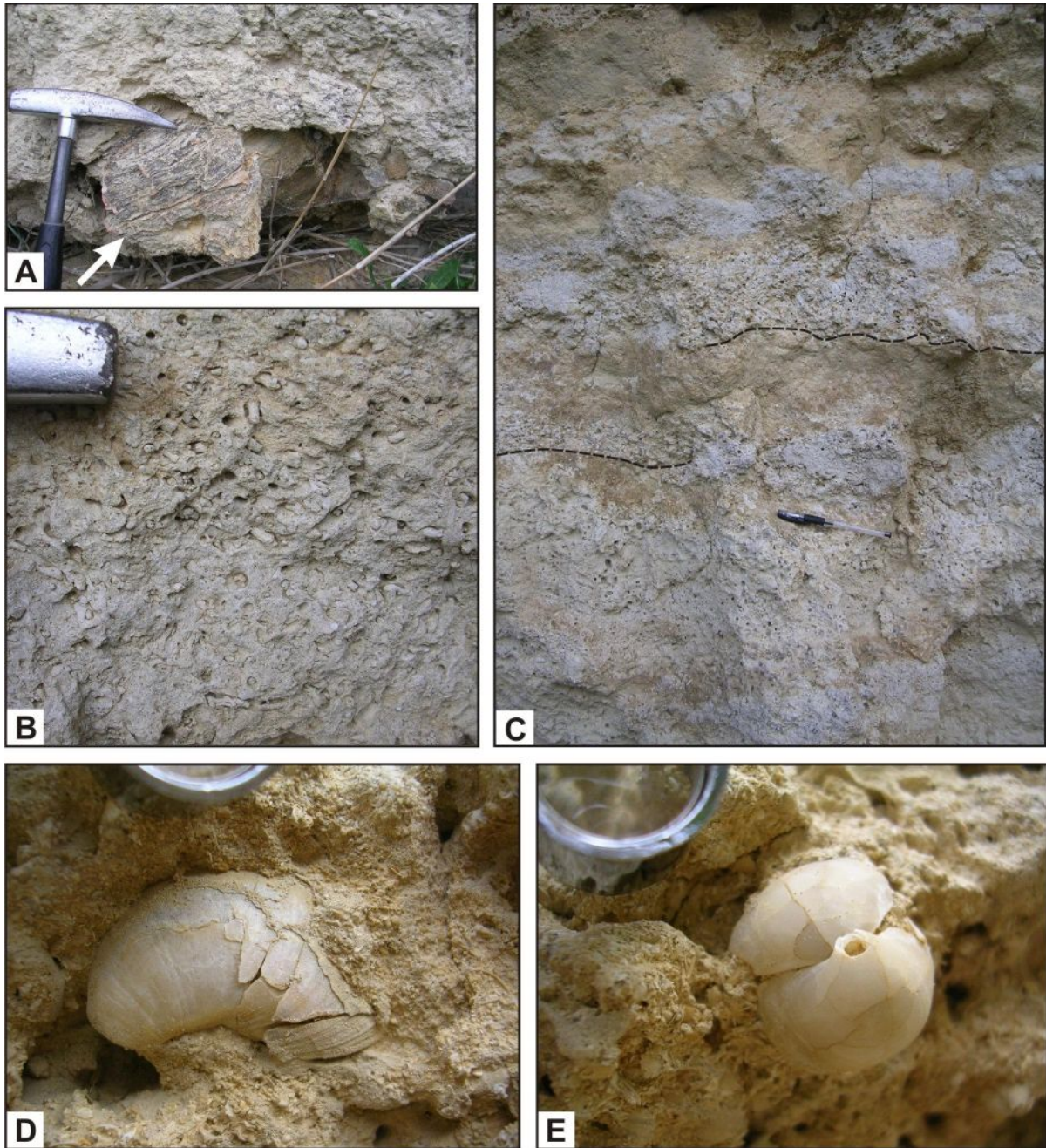


Figure 8. Detail of a well-rounded large clast (white arrow) derived from the crystalline basement within the biocalcarene of the lowermost Stratal unit *a* of cycle R2 (La Montagna 1 section in Figure 5; hammer for scale, about 30 cm). (B) Detail of the corals within Stratal unit *a* and (C) view of their stratal organization (dotted lines indicate the strata bases). (D and E) Close-up view of *Terebratula* with articulated valves within the uppermost Stratal unit *b* along the La Montagna 1 section (lens as scale is about 5 cm diameter).

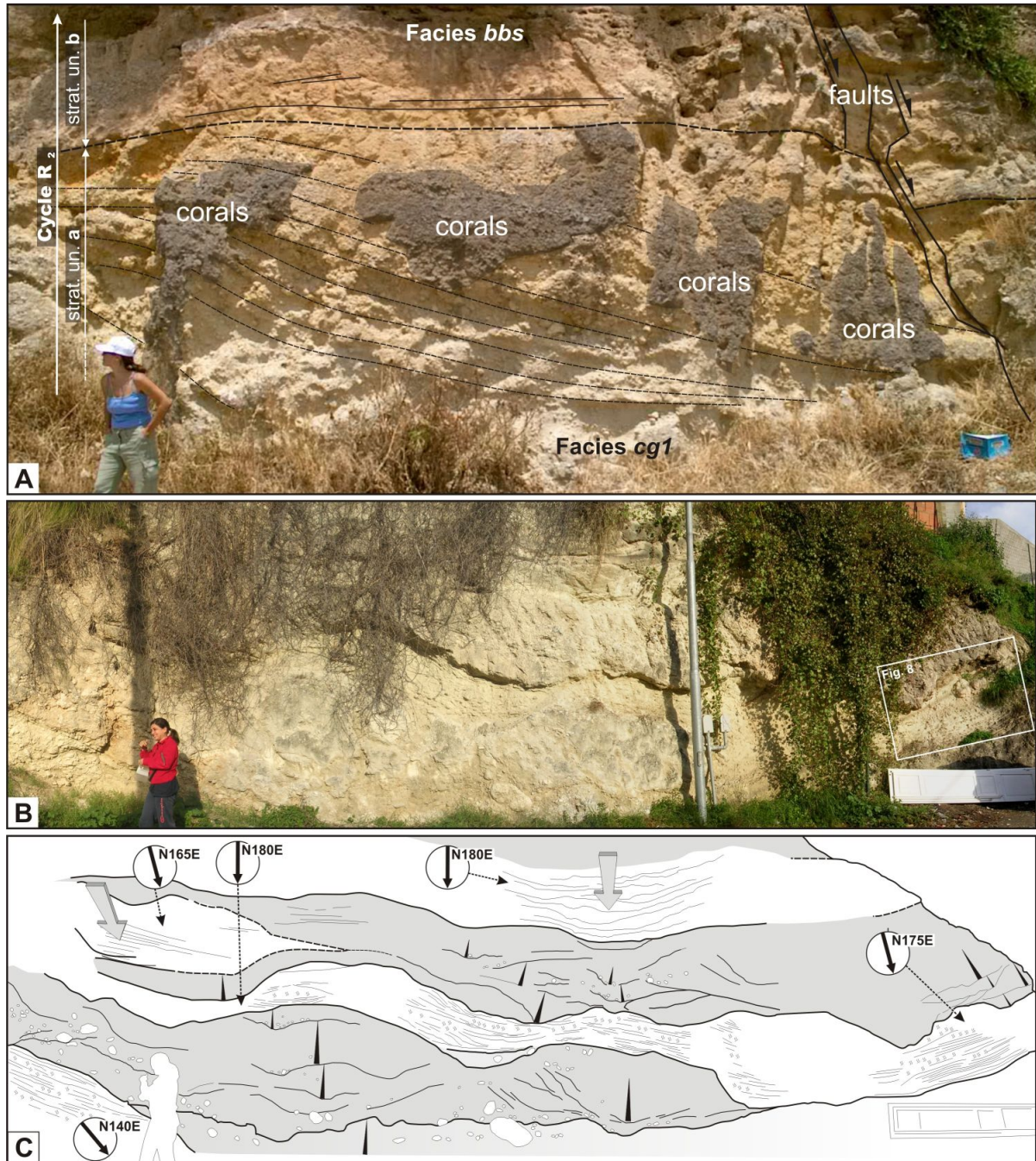


Figure 9. Outcrops of cycle R2 at La Montagna 2 section. (A) Lowermost part shows sigmoidal strata of pebbly sandstones (Stratal unit *a*, facies *cg*) interrupted by coral colonies. This wedge-shaped unit is overlain by Stratal unit *b*. (B) Photomosaic of a well-exposed section showing facies architecture at the base of Monte Spalatarà locality. Here facies association *cc* crops out (first author as scale). (C) Line-drawing of the previous photograph showing alternating packages of multiple debris flow channelfills (facies *cc1*) and cross-stratified tidal dunes (facies *cc2*). Grey arrows indicate the migration directions of dunes, whilst black arrows indicate fining-upwards trends within the channelized deposits.

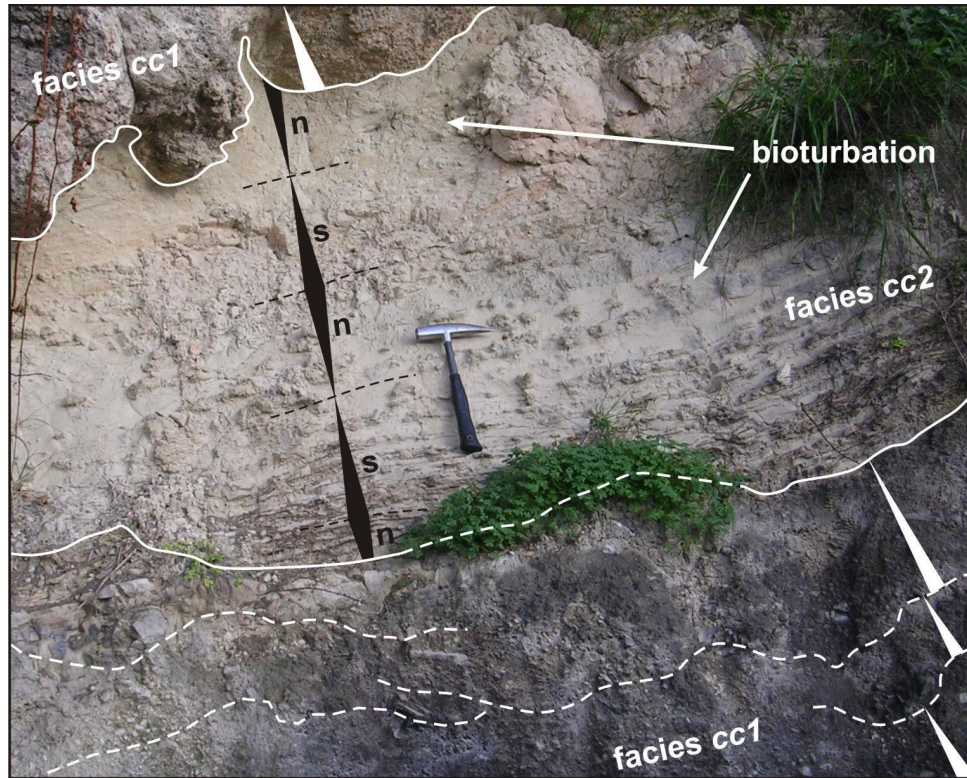


Figure 10. Close-up view of the outcrop in Figure 9B. White lines separate the two lithofacies of facies association cc at the base of Monte Spalatara section. Facies cc1 consists of multiple grain flow channelfill deposits, containing rock fragments recycled from the pre-Pleistocene bedrock (white arrows indicate normal grading). Facies cc2 consists of cross-laminated tidal dunes composed of bundles of coarsening- and fining-upwards foresets (migration direction is somewhat normal to the outcrop surface), recording repeated neap/spring (n/s) tidal cycles. Bioturbation is widespread. Note loading structures at the base of the successive grain flow strata.

4.1.2. Stratal unit b

The previous Stratal unit *a* passes upwards to Stratal unit *b*, which extensively crops out at San Filippo, La Montagna and Monte Spalatara (Figure 1), showing significant lateral variations in thickness (Figure 5). This unit exhibits a single facies association *bc* which is in turn composed of facies *bss* and subordinately facies *ic*. Facies *bss* consists of a 15–20 m thick well-stratified alternation of yellowish grainstones, rudestones and packstones (Figure 5), containing sparse mm-sized quartz particles. The bioclastic fraction is represented by well-sorted skeletal particles, derived from debris of bivalves, gastropods, brachiopods, echinoderms, bryozoans, ostracods, barnacles, corals and red algae. Centimeter-thick interlayers of silt to fine-medium sand are also present, mainly consisting of quartz, feldspar and glauconite grains. The occurrence of both bioclastic and siliciclastic fractions allows us to define these sediments as ‘mixed’ sandstones [28] or ‘hybrid arenites’ [29]. In the San Filippo section (Figures 11A and 11B), facies *bss*

shows abundant small-sized brachiopods, well preserved and sometimes with articulated valves. Here, the unit is organized into a regular repetition of centimeter-thick beds characterized by tabular geometries, with foreset lamination showing unidirectional palaeocurrents (N160–N180E). Very intense bioturbation often hampers the recognition of other primary sedimentary structures (Figure 11C).

Basinwards, sediments of Stratal unit *b* are truncated by a U-shaped, 5–6 m deep channel incision (Figure 5), filled with intraformational, chaotic calcarenitic and metamorphic clasts, up to 35 cm in diameter (facies *ic*). The axis of the channel is downdip oriented, according to the palaeoslope direction of the system.

4.1.3. Stratal unit c

The topmost part of depositional cycle R2 is represented by Stratal unit *c* (Figure 5). This unit consists of well-stratified, deeply bioturbated, bioclastic siltstones up to 10–12 m thick, containing few loosely packed thin lenses

of bioclastic fine sands (facies *bs*) and dispersed well-preserved fossils. The basal contact over the underlying Stratal unit *b* is well exposed. This surface is characterized by a 30–50 cm thick, in situ to near situ exceptionally abundant shell concentration of centimeter-sized skeletons of articulated brachiopods *Terebratula*. (Figures 12A and 12B). Upwards, thinner shell concentrations occur, alternating with fine calcarenitic intervals. The uppermost

part of the unit is characterized by wavy erosion surfaces, with a relief of 15–20 cm, filled with shell fragments. No other current or wave sedimentary structures occur. This unit is bounded at the top by a surface of modern exposure (San Filippo) or it is overlain by the prograding fan deltas of the late Middle Pleistocene Messina Gravels and Sands Fm (La Montagna and Monte Spalatarà) (Figure 1).

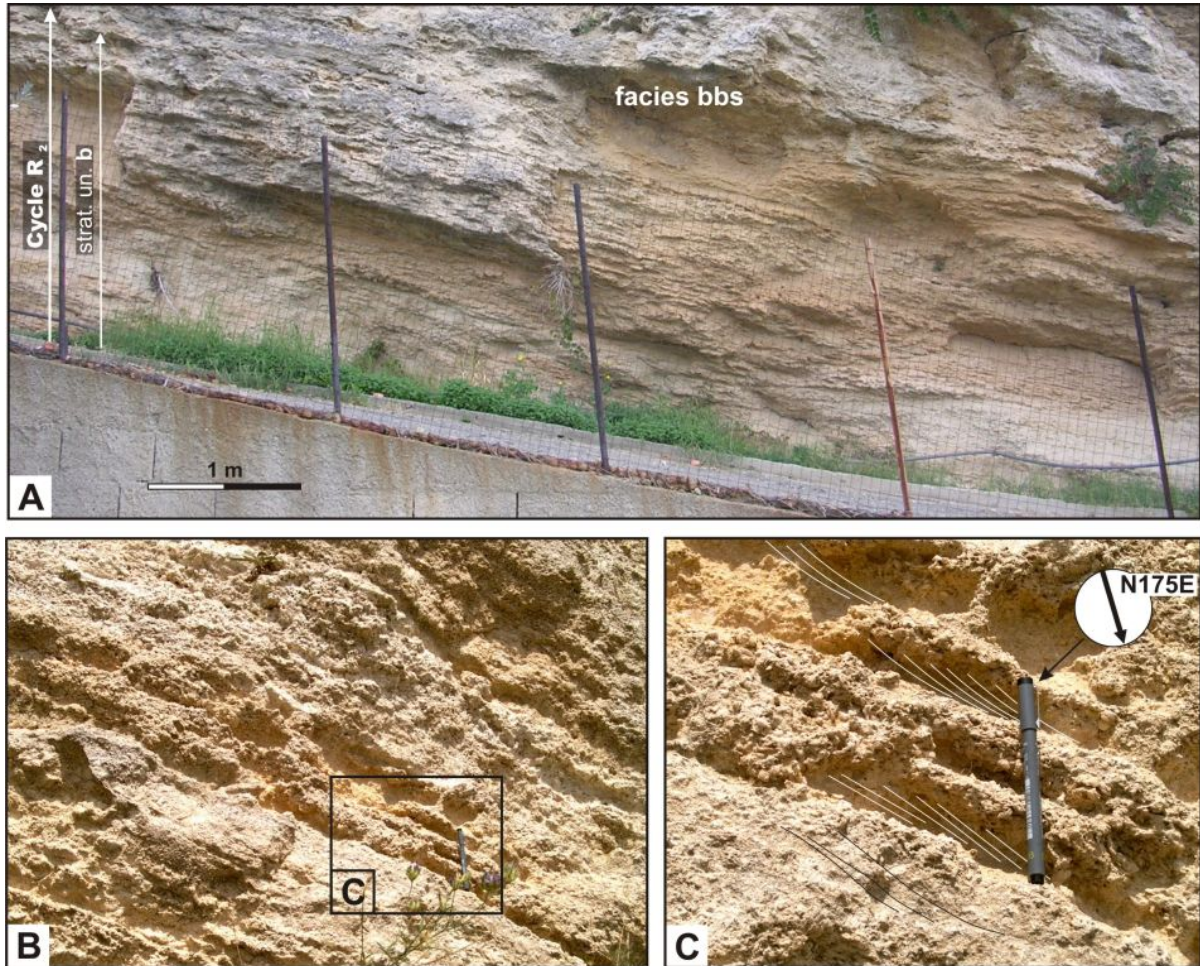


Figure 11. (A) Low-angle cross-lamination of the biocalcarenes of Stratal unit *b*. (B) Detail of the previous photograph. Note the tabular cross-strata and the abundance of the bioclastic fraction. (C) Close-up view of the facies *bbs* showing uni-directional packages of foresets.

4.2. Cycle R3

Depositional cycle R3 crops out in the NE sector of the study area (Figure 1). Here the litho–stratigraphic characteristics of this succession appear very similar to those of the underlying cycle R2, and for this reason the two

diachronous cycles R2 and R3 were so far considered as coeval in the past [32, 33]. The nannofossil content indicates that cycle R3 is referable to the MNN19f biozone (Figure 3), characterized by the occurrence of *Gephyrocapsa* sp.3 [73], whose First Occurrence approximates the

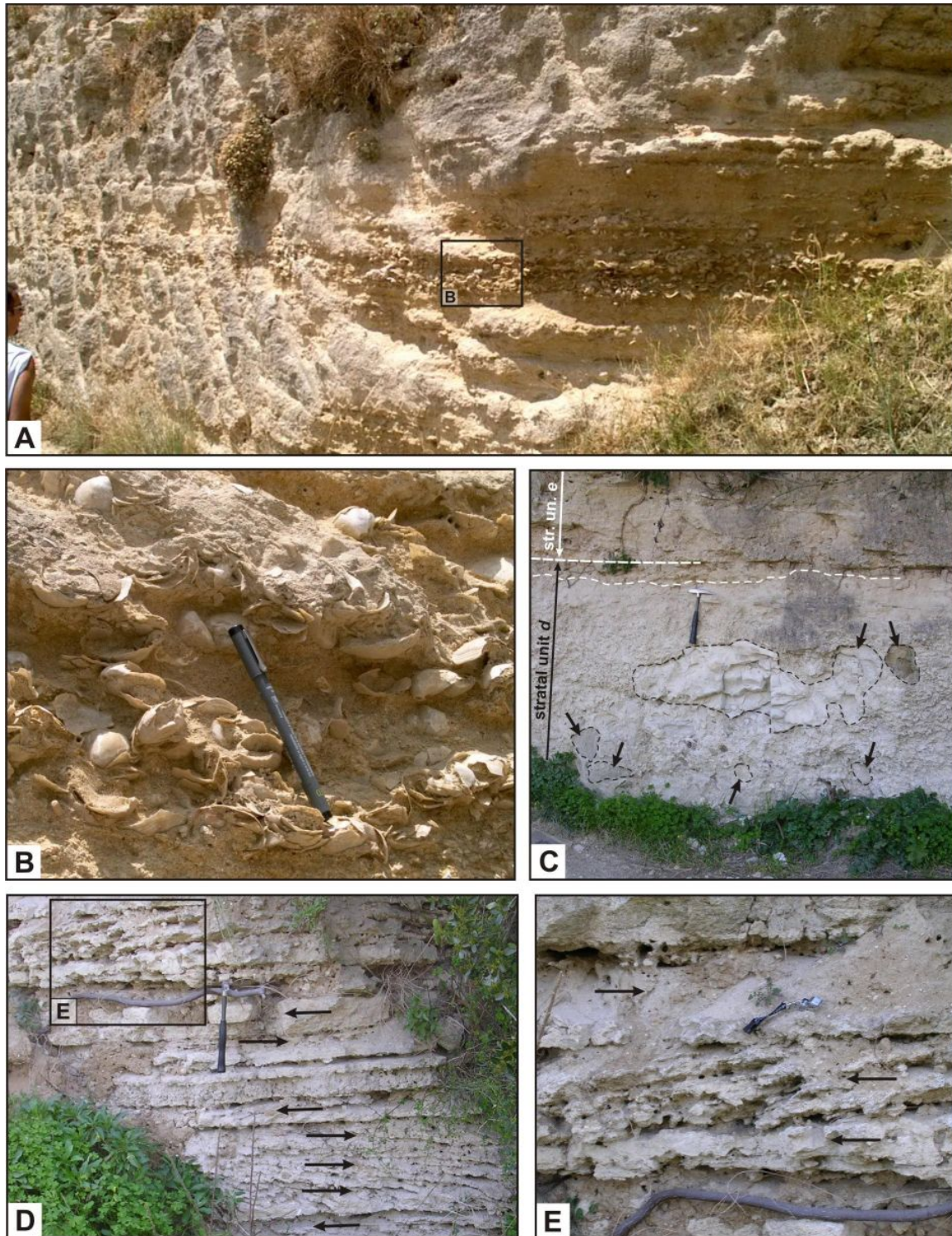


Figure 12. (A) Shell bed composed of *Terebratula* valves, marking the contact between Stratal units *b* and *c* within cycle R2 (mfs) (top of La Montagna 2 section in Figure 5). (B) Detail of the previous photograph. (C) Facies *df* at the base of cycle R3 (Scoppo section). This chaotic debris flow deposit consists of recycled clasts of pre-Pleistocene bedrock and cycle R2 sediments (black arrows, the biggest white block derives from Lower Pliocene Trubi Fm). (D) Strata of cross-laminated biocalcarenites pertaining to Stratal unit *e*. Note opposite-dipping (arrows) foresets (herringbone structures) suggesting the influence of tractional currents induced by ebb/flood tidal cycles. (E) Detail of the previous photograph.

Middle Pleistocene basal boundary [76]. Cycle R3 spans from 0.99 Ma (base of the MNN19f biozone [75]) to 0.58 Ma (Last Occurrence of *Gephyrocapsa* sp.3 [75]; see Table 1 for further details).

Cycle R3 overlies the deformed pre-Pleistocene bedrock through an irregular discontinuity surface (ts^{ll} in Figure 6) and is organized into two main stratal units, *d* and *e*. The succession shows a deepening-upwards trend indicated by sudden vertical changes in the sedimentary facies.

4.2.1. Stratal unit *d*

This unit represents the lower interval of Monte Banditore and Scoppo sections (Figure 6), and it is mainly represented by pebbly sandstones lapping on the pre-Pleistocene block-faulted substrate (San Pier Niceto and Trubi fms).

Stratal unit *d* is represented by facies association *sc*, which is composed of three facies: *smb*, *dd* and *df*. The first two are observable at the base of Monte Banditore. Facies *smb* consists of laminated siltstone and microbreccias forming tabular beds up to 0.5 m thick (Figure 7C). Mm-sized bioclasts are sparsely present within the siltstone and where present, are organized to form flat laminations, frequently obliterated by bioturbation. Locally, thin sandy intercalations with ripple cross laminations occur. Facies *dd* is represented by chaotic, coarse-grained arenitic to conglomeratic strata, 1–1.5 m thick and frequently reverse graded. These strata include large clasts, up to 0.5 m in diameter of metamorphic, arenaceous, marly and biocalcarenic rocks, immersed in a fine bioclastic matrix. Biocalcarenic fragments yield nannofossil assemblages similar to those found in the R2 sediments, and thus referable to the Early Pleistocene.

Northwards, these facies pass laterally to facies *df*, which occurs at the base Scoppo section (Figure 12C). Facies *df* consists of chaotic, amalgamated, 4–7 m thick beds of coarse sediments. The coarser fraction is represented by large mudstone blocks, containing abundant Early Pliocene nannofossils (*Amaurolithus delicatus*, *Hellicosphaera sellii*, *Discoaster pentaradiatus* among others). Subordinate arenaceous and metamorphic clasts are also present. The clay matrix yields rich and well-preserved nannofossil assemblages of the Middle Pleistocene MNN19f biozone (Table 1), with abundant open-marine forms such as *Pseudoemiliana lacunosa*, as well as typical Pleistocene circalittoral to bathyal benthic foraminifers such as *Hyalinea baltica*, and planktonic foraminifers such as *Turborotalia truncatulinoides excelsa*.

4.2.2. Stratal unit *e*

Stratal unit *e* developed over the previous Stratal unit *d* on a flat depositional surface. This unit mainly con-

sists of stratified mixed sandstone and siltstone, where the bioclastic fraction is represented by fragments of corals, serpulids and sponges, and the siliciclastic fraction by small clasts of quartz (facies *cbc*). Skeletal material appears ubiquitously disarticulated, fragmented and commonly rounded and polished, due to both biological and physical processes of degradation. Sediments are organized into tabular beds a few centimeters thick, containing angular to tangential foresets (Figures 12D and 12E). Palaeoflows display directions ranging from N95°E to N300°E, so that repeated vertically-stacked foresets form herringbone structures (Figures 12D and 12E). Bioturbation is widespread. Randomly, thin lenses of granules and small-sized pebbles occur at different stratigraphic intervals. This facies, up to few meters thick, is abruptly truncated at the top by the erosional surface, marking the base of the overlying Messina Gravels and Sands Formation (Figure 6).

5. Discussion and interpretation of the depositional setting of cycles R2 and R3

Cycle R2 is organized into a series of wedge-shaped coastal bodies, slightly inclined seawards. Although syn- and post-depositional tectonic displacements affected the entire area, facies arrangement indicates that this inclination is depositional. Facies assemblages, as well as biofabric and preservation quality, suggest a shallow mixed siliciclastic/carbonate ramp setting, most of which developed below the fair-weather wave base, with a weak deepening trend. The absence of clinform geometries and the rapid lateral facies changes indicate that the lower Stratal unit *a* is the result of coastal sedimentation along a gentle seaward dip ramp. This ramp was formed by a narrow, poorly developed beach face, rapidly passing seawards to a subaqueous shoreface (Figure 13A). The semi-organized breccia, rich in encrusting organisms and corals (facies association *pb*), represents deposition at the toe of sea cliffs. These deposits accumulated by debris flows and debris falls due to events of rock failure from coastal paleocliffs. Molluscs and sponge borings affecting both boulders and cliffed substrate indicate that rock failure accumulated in the transition from beach face to upper shoreface. These facies may develop in an environment similar to that characterizing some present-day coasts, where steep (cliffed) shorelines exhibit smooth nearshore profiles and a 'reflective' hydrodynamic domain [82]. In such settings most waves break directly against the beachface, and wave energy reflected from the beach face often propagates offshore by refraction producing a 'resonance' of water move-

ment along the beach face [83]. Abundant bedrock-derived clasts occurring at the base of the palaeocliff, and representing the 'back-edge' of the coastal system, probably originated from fault-induced sea cliff collapses. However,

no flexure or deformation of the conglomerate beds occurs to confirm syn-depositional tectonic activity of faults affecting the pre-Pleistocene substrate.

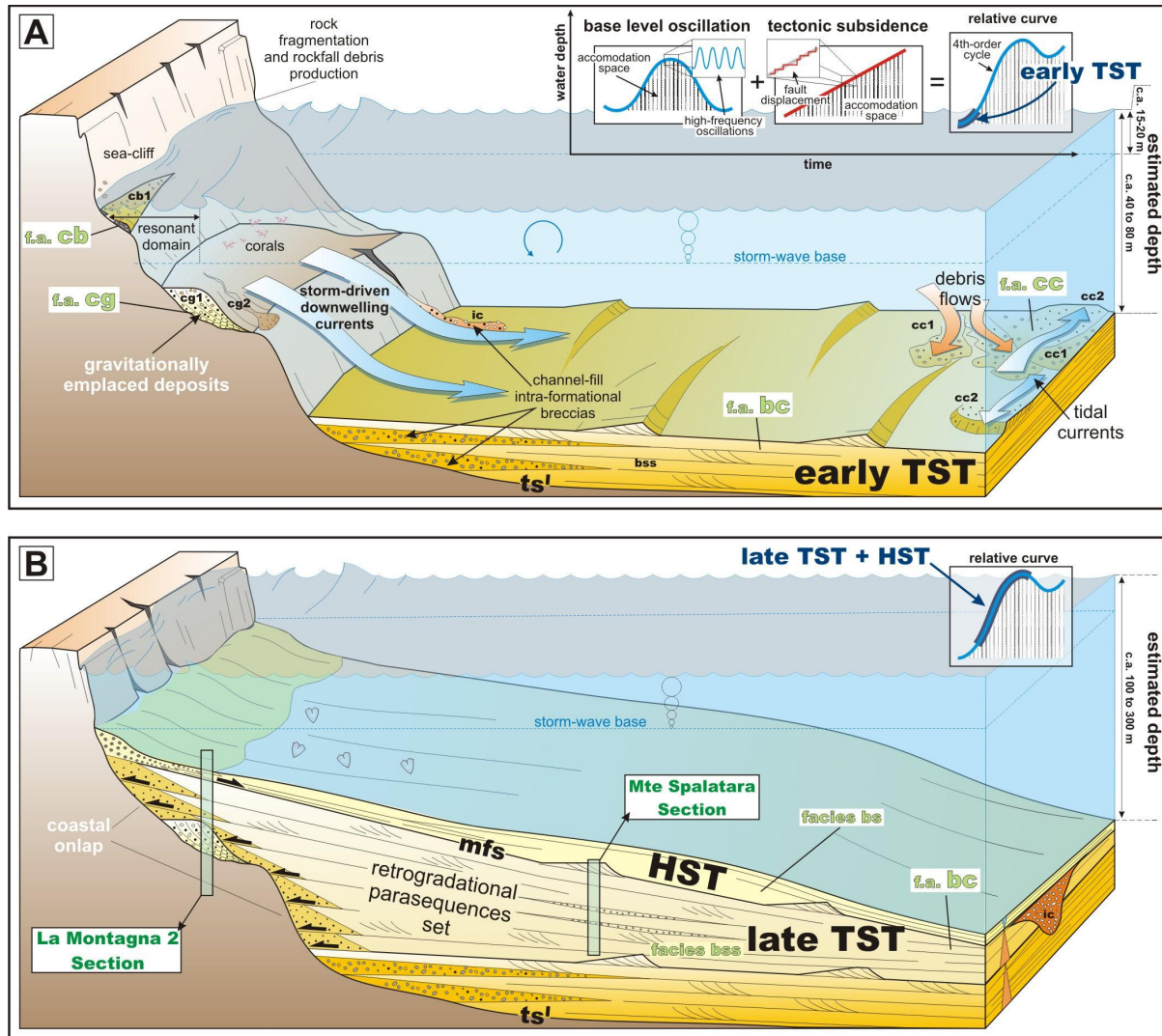


Figure 13. (A) Depositional 3D model inferred during the early stage of deposition of cycle R2 (early TST on the relative sea-level curve). The steep depositional profile inhibited the development of proximal facies. The incidence of waves against the sea cliffs might produces a 'resonant' domain in the foreshore zone, generating downwelling currents migrating offshore along the sea bottom and influencing the deepest sedimentation (facies association bc). In the distal part of the depositional model, the emplacement of debris-flow deposits, derived from an adjacent steep margin, alternated with tidal dunes migrating parallel to the palaeo-shoreline (facies association cc). (B) Development of the depositional system during the late relative sea-level rise and subsequent highstand (upper part of cycle R2). Sedimentation took place with the development of a set of retrogradational parasequences (testifying short-term eustatism) lapping against a steep transgressive surface (see the stratigraphic locations of the sedimentological logs shown in Figure 5). The curve of relative sea-level oscillation can be considered as the sum of the eustatic sea level changes and the tectonic subsidence [113]. See text for details.

Although previous interpretations have attributed the coral assemblages from the study to circalittoral/bathyal and bathyal environments e.g.: [5, 84], the described sedimentary structures suggest shallow-water conditions for deposits of Stratal unit *a*. This apparent contradiction between the palaeological and sedimentological data was also noted by [24] for an analogous succession in the Tyrrhenian sector. According to the authors, similar discrepancies can be attributed to the high water turbidity, especially for engulfed coastal conditions, which would reduce the penetration depth of light and affect the bathymetric distribution of local biocoenoses. Large volumes of sediments in suspension can be entrapped in bays by the action of waves or longshore currents, reducing light conditions at the sea floor. Such conditions may simulate depths greater than the reality thus favoring the development of faunal assemblages usually living in deeper environments [24]. In addition our interpretation is supported by recent findings that documented a wider bathymetric range for *Lofelia pertusa* and *Madrepora oculata* assemblages (33–463 m) [85].

Basinwards, facies association *pb* is replaced by debris-flow deposits (facies *cc1*), probably shed from the marginal areas following collapse of fault-controlled palaeocliffs. These deposits are intercalated with sandy tidal dunes migrating parallel to the palaeoshoreline (facies *cc2*). Bundling of foreset laminae (Figure 10) suggests neap/spring tidal cyclity. This stratigraphic arrangement is very similar to that described for Plio-Pleistocene deposits on the Calabrian side of the Messina Strait and interpreted as typical tide-influenced sedimentation of a palaeo-strait margin [86]. The average orientation of the proto-Messina Strait axis was NNE–SSW [1, 2], and tidal currents were expected to mirror this direction. The different trend of the tidal palaeoflows (N140° E to N 180° E), recognized in the foresets of the basal intervals of the succession, presumably suggests a deeply engulfed coast, marginal to the axial part of the strait. Therefore, the observed facies can be considered as recording sedimentation in the sublittoral environments of the proto Messina Strait.

This coastal setting evolved transgressively to biocalcarene-dominated lower shoreface conditions (stratal units *a* and *b*, inferred paleo-depth interval: 40 to 80 m), followed by open-marine siltstone (Stratal unit *c*, inferred paleo-depth interval: 100 to 300 m) (Figures 13A and 13B).

Lower shoreface setting of Stratal unit *b* is suggested by the low amount of wave- and storm-induced sedimentary structures. These are replaced upwards by current-induced structures, mostly tabular cross-beds, which can be interpreted as a product of tractional downwelling

flows. Such features confirm a ramp-type depositional setting during its transgressive stage, characterized by the dominance of storm-driven downwelling and offshore-directed currents (facies *bbs*), and gravity-driven deposits (facies *ic*) (Figure 13B). According to the skeletal components of the bioclastic fraction (facies *bbs*), a foramol assemblage (sensu [87] and [30]), typical of temperate to cool water seas, can be hypothesized [31]. The related carbonate factories characterize unrimmed, open seaward-sloping shelves, dominated by the influence of waves and storms and subordinately by gravity-driven processes [88] in areas characterized by cool and/ or nutrient-rich waters [31].

The internal organization of the lower, biocalcarene-dominated Stratal unit *b* and its association of sedimentary structures indicate the occurrence of re-sedimentation processes, producing gravity-driven mass flows (debris falls and debris flows) that propagated along a steep seabottom profile. The ramp top represents the shallowest environment. The bioclastic fraction that originated in this setting was promoted by the proximity to photic zone and by an abundance of land-derived nutrients ('non-tropical carbonates' of [88]). In the same environment, the larger part of the siliciclastic fraction of sediment deriving from the rivers or littoral drift accumulated and mixed with the carbonate skeletal fraction. These mixed sediments were remobilized by storm-induced downwelling flows, giving rise to gravity flows as the ramp deepened basinwards.

The abundance of the fine-grained, bioturbated matrix that characterizes the topmost Stratal unit *c* suggests deposition below the fair-weather wave base, in an environment with perennially abundant sediment suspension rich in silt and very fine skeletal sand. The bioclastic interlayers of facies *bs* and the rare wavy erosional surfaces can be attributed to storm events, implying an offshore-transitional environment.

The depositional setting of cycle R3 was similar to depositional setting of the older cycle R2. Differences can be found in the lower part of cycle R3 (Stratal unit *d*), where clasts derived from the pre-Pleistocene substrate occur. These are mainly represented by marls of the Trubi Formation, as revealed by the Early Pliocene nannofossil assemblages and, subordinately, by arenites of the San Pier Niceto Formation and metamorphic rocks. The recycling of cycle R2 sediments is confirmed by the nannofossil content of the calcarenitic clasts which revealed an Early Pleistocene age. This evidence suggest incipient uplift and erosion of the marginal areas during the initial stage of the Middle Pleistocene transgression e.g.: [89]. Stratal unit *d* of cycle R3 represents an open-marine depositional setting (inferred paleo-depth interval: 300 to 500 m), in which gravitational events (rock falls and de-

bris flows) tend to affect the deepest environment. The uppermost part of cycle R3 (Stratal unit *e*, inferred paleo-depth: >500 m) indicates sedimentation in a ramp setting, in which siliciclastic/bioclastic cross-stratified sandstones are characterized by an upward increase in abundance of tide-dominated sedimentary structures.

Tidal signal is recognizable in both cycles R2 and R3, although it is represented by two different types of sedimentary record. The lower portion of cycle R2 exhibits 2D tidal dunes, up to 4 m thick (see Figure 9C), whose internal architecture shows neap/spring bundling of laminae (see Figure 10). These dunes display uni-directional palaeoflows and indicate chiefly uninterrupted currents moving in the relatively deep part of the proto-Messina Strait.

In contrast, the tidal signal of cycle R3 consists of vertically-stacked tabular foresets, with thickness ranging from 0.2 up to 0.5 m, showing alternating palaeoflow directions. These two different types of tidal facies are probably related to two different depth conditions of the strait: large 2D tidal dunes currently occur in the deepest zones of the strait [70], whilst reverse flood-ebb currents can be more easily recorded in shallower environments of the tide-dominated marine system [90]. Thus, the differences in tidal signature possibly indicate that the Messina Strait experienced different hydrodynamic conditions related to evolving depth from the Early to Middle Pleistocene.

Similar depositional settings were described, interpreted and debated for other coeval and older successions. Most of the proposed models represent wave- or storm-dominated depositional settings e.g.: [15, 21, 25, 91–94]. In contrast, the study sections do not fit the published depositional models in detail, because the observed facies do not show any trace of swaley or hummocky cross-stratification that could be attributed to wave- or storm-influenced depositional environments [21, 88, 92].

The facies examined in this study show ripple and mega-ripple cross-stratifications with basinward-oriented palaeocurrents, indicating constant offshore-directed currents. As all these structures occupy the uppermost part of the model and, therefore the sector immediately adjacent to the steep beach, it is possible that the bottom profile did not provide enough space to record and preserve wave- and storm-influenced facies. Waves might have played an important role in the coastal hydrodynamics: on impact with the steep coastal profile (cliff), waves may have produced reflection (rather than dissipation) of energy and consequent wave-driven downwelling currents (along-ramp geostrophic flows). The palaeo-bottom depositional profile may have pertained to a steep palaeo-coast, characterized by cliffs and poorly developed beach deposits (or 'pocket beaches'). Thus the steep deposi-

tional profile may have inhibited the development of clinoforms [26]. Similar depositional models were proposed by [26] and [22].

6. Sequence stratigraphic interpretation of cycles R2 and R3

The facies succession observed in the analyzed sediments indicates that they represent two transgressive cycles (R2 and R3), both bounded at the base by evident angular unconformities (Figure 2B). Cycle R2 is bounded at the top by a further unconformity surface, locally overlain by the late Middle Pleistocene fan deltas of the Messina Gravels and Sands Formation. The same deltaic deposits lie at the top of cycle R3 through an erosional surface which, consequently, can be regarded as a 'regressive surface of marine erosion' (rsme in Figure 6).

Both cycles R2 and R3 evolve from Transgressive System Tract (TST, Stratal units *b* and *d*) to Highstand System Tract (HST, Stratal units *c* and *e*) (Figure 4) and lack their Lowstand System Tracts.

The transgressive character of each cycle is evidenced by the deepening trend indicated by the upward fining of the sedimentary facies and by a substantial decreasing of the siliciclastic fraction in the upper intervals. During transgression, the coastline moves landward and the shelf area typically enlarges. This could be accompanied by a storage of large quantities of sediment in the alluvial and coastal plain environments, resulting in reduced sediment influx to the basin. The deposits that record the late stages of the transgression are indeed represented by fully marine bioclastic fines, characterized by a consistent decrease in the siliciclastic fraction.

Transgressive deposits culminate in a surface or zone of maximum flooding. In sequence stratigraphic reconstructions maximum flooding surface (mfs) is considered a key surface, generally easily detectable in outcrops and cores, and representing the downlap surface of the overlying regressive deposits [95, 96]. Downlap is not evident in the study area because the study sections expose the distal part of the stratigraphic sequence, which exhibits a very gentle clinoform dip. In these distal areas the clinoforms appear as subhorizontal surfaces of open marine deposition. Downlap geometries could theoretically be identified from large outcrop views, which are absent in the study area. The mfs that separates the TST from HST is here represented by a sudden change in the sedimentary facies from shoreface, coarse grained, mixed sandstones to offshore siltstones (Figures 7A and 7B). In cycle R2 this surface is also marked by a relevant concentration of brachiopod shells of *Terebratula* genus (Figures 12A and 12B).

On the contrary the mfs that characterizes cycle R3 is not associated with a shell bed and, in our interpretation it coincides with the top of Stratal unit *d* (Figure 12C). In fact, from this point upwards, a weak shallowing trend of the succession is observable, thus indicating a relatively stable sea-level.

The biocalcarenite succession of cycle R2 (Stratal unit *b*) represents an ‘accretionary transgression’ (sensu [97]) that typically characterizes steep coastal margins during relative sea-level rises. Transgressive deposits may develop above the wave ravinement surface in steep and high-sediment-supply settings (transgression *T – D* of [98]). In places, where faulting creates steep ramps such as the study area, the transgressive deposits are usually much thicker than in other, gently-inclined coastal areas, because the eroded and newly supplied sediment is deposited locally without significant dispersion across the shelf area. Cycle R2 biocalcarenites can be regarded as a set of higher-order ‘amalgamated parasequences’ [99, 100], arranged in mostly retrogradational pattern. Each parasequence records deepening trend, accompanied by slight facies changes. Minor flooding surfaces are present at the top of each parasequence, marked by thin layers of brachiopods (‘condensed downlap shell bed’ [101], ‘type B shell bed’ [102], or backlap shell bed’ [103]) indicating minor stillstands of the relative sea level.

Parasequences of cycle R2 show upward deepening with no shallowing-upward trends (regressions). Thus, they differ from the classical, progradational parasequences related to shoreline advancement, that are readily recognizable by a shallowing-upward signature of component facies [104, 105]. Nevertheless, as argued by [98], and documented for analogous Neogene successions of Southern Italy [24, 106], transgressive trends can be recognized based on evidence of a landward shift of facies (retrogradation). However, this retrogradational facies arrangement is better developed along gently-inclined coastal margins and is less apparent along steep coasts such as that of the study area (Figure 13B). Cycle R2 internal arrangement seems to be in contrast with the classical models, where sea-level rise occurs according to steps of rapid rises and minor sea-level stillstands. In fact, such a mechanism produces alternation of coastal retrogradations and minor progradations, despite a longer-term, landward stepping of the shorezone [107]. Thus, the absence of progradational patterns within the R2 succession suggests that the recorded transgressions might have been continuous, or without any significant pause during the relative sea-level rise.

Parasequences of cycle R2 regularly alternate displaying no significant bed-thickness differences and facies variations to each other. Such vertical repetition can-

not be generated by a non-cyclical factor (e.g. tectonics), which usually produces a random signal in the sedimentary record. Because cycle R2 deposited during the Early Pleistocene and this time interval was characterized by a dominant periodicity of 41 ky in glacial oscillations (see $\delta^{18}\text{O}$ curve in Figure 3) ([108–110] and references therein), we can consider the regular signal recorded by parasequences as an effect of short term eustatism. Consequently, the general transgressive trend of cycle R2 reflects the increase in accommodation space produced by fault displacement with the superimposition of high-frequency eustatic sea-level oscillations. The sedimentary succession does not record any effect of the falling stages which occur during eustatic high-frequency cycles, because the rate of tectonic subsidence exceeded the magnitude of the short-term sea-level falls. For this reason, the general transgressive trend may be considered the result of an uninterrupted relative sea-level rise induced by tectonics.

Vertically-stacked parasequences are not evident in cycle R3 because the TST is here represented by chaotic to poorly-organized deposits (Stratal unit *d*). The deposition of cycle R3 occurs most likely after the “mid-Pleistocene transition” [111], that marks the onset and establishment of 100 ky glacial cycles. As shown by the $\delta^{18}\text{O}$ curve (Figure 3), the past 900 ky or so, are characterized by “asymmetric” (short, abrupt deglaciation and long, gradual glaciation phases), higher-amplitude and longer-term glacial cycles [112]. We may suppose that cycle R3 deposited during a deglaciation phase, which caused an amplification of the tectonic subsidence effect. This resulted in a higher amplitude of the general transgression, as suggested by the deeper environments indicated by the uppermost facies associations (Stratal unit *e*).

Tectonic subsidence, related to the movement of active faults, usually occurs through steps producing short discontinuous displacements, also associated with seismic events. These steps are not included in the studied sedimentary successions as the accumulation rate probably occurred over too long a time-scale to record short-term tectonic episodes. Accordingly, in a sequence stratigraphic reconstruction the tectonic subsidence can be expressed as a ‘straight’ line (inset in Figure 13A) in the estimation of the resultant curve of the relative sea-level oscillation [113].

7. Proposed tectonic model for the deposition of cycles R2 and R3

Cycles R2 and R3 mainly directly lie upon the pre-Pliocene substrate. The Lower Pliocene deposits (Trubi

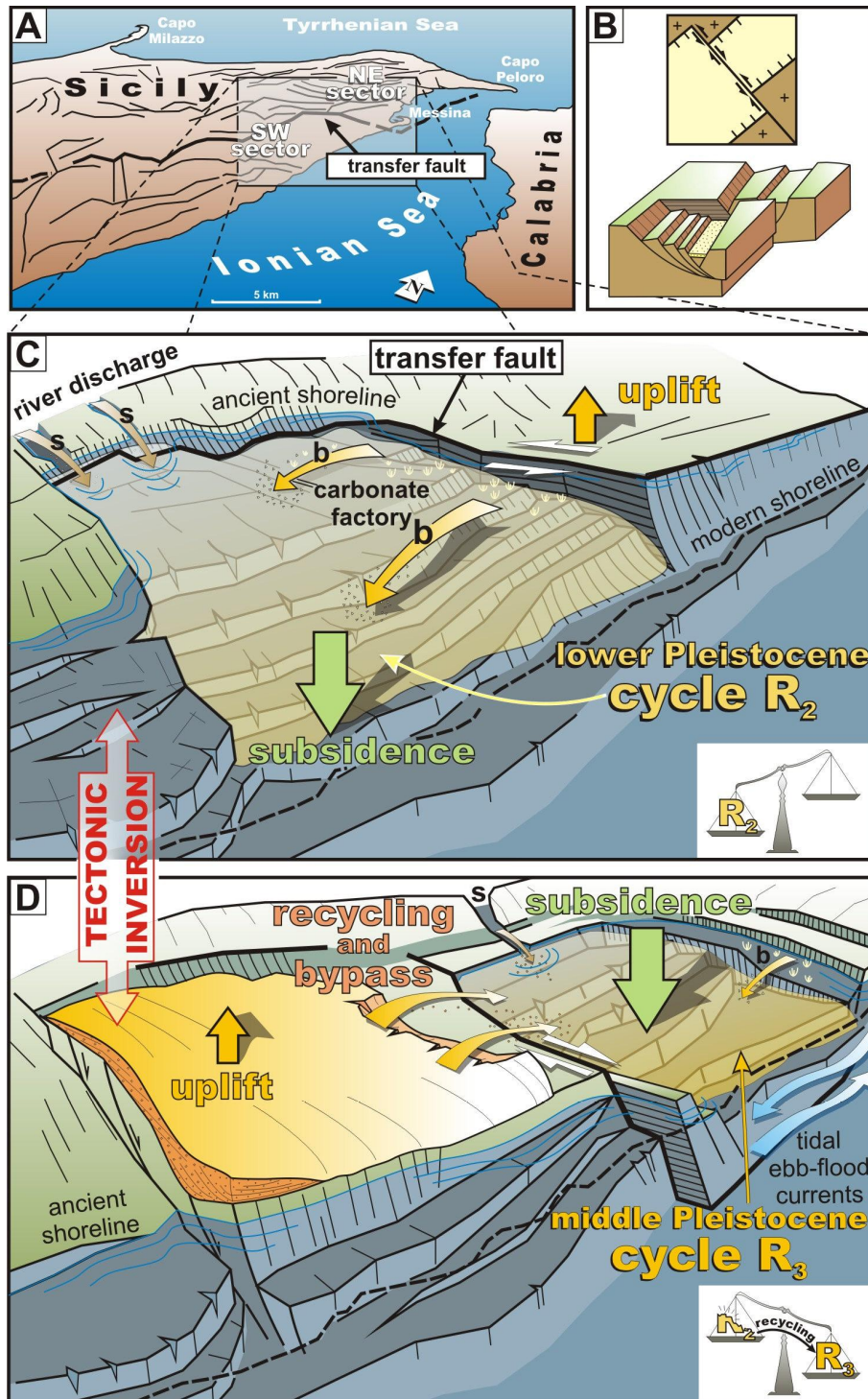


Figure 14. (A) Perspective view of NE Sicily and the main tectonic lineages [33]. Rectangle indicates the location of the study area subdivided into the SW and NE sectors. (B) Model of a transfer fault system (modified after [116]). Movement sense changes along strike of the same transfer producing the offset of depocenters parallel to the rift opening. (C) During the Early Pleistocene, the activity of the transfer fault system with left strike-slip movement may have produced local subsidence, where cycle R_2 developed, fed by siliciclastic (s) and bioclastic (b) sediments. (D) The progressive evolution of this fault system caused tectonic inversion accompanied by right strike-slip movement: the SW sector was uplifted, cycle R_2 underwent deep erosion and cannibalization and the creation of new accommodation space in the NE sector favored the sedimentation of cycle R_3 . At this time, ebb-flood tidal currents started to influence the sublittoral sedimentation, anticipating the opening of the adjacent Messina Strait.

Formation) occur discontinuously in very thin outcrops. The absence of Middle–Upper Pliocene sediments which occur frequently along the Tyrrhenian side of NE Sicily (depositional sequence R1 [22]), indicates that this margin of the Ionian basin was uplifted during the Middle Pliocene to the earliest Pleistocene.

The two cycles appear confined to two, SW and NW, sectors of the same coastal segment and are separated from each other by a WNW–ESE-oriented fault. This fault belongs to the Ionian segment of the ‘Calabro–Siculo Rift System’ [34, 53, 54], which since the Late Pliocene, gave rise to the distinct palaeogeography of the study area. This was characterized by a series of semi-confined gulfs, controlled by shore-parallel normal faults and associated minor, perpendicular strike-slip faults [34, 53, 54] (Figures 1 and 14A).

The two depocenters subsided during two successive stages, inverting their position and role during sedimentation. This mechanism may have been related to the tectonic activity of a transfer fault system, which caused inversion of different subsiding areas during its evolution. Theoretically, a transfer fault system [114], comprises orthogonal faults which accommodate differences in strain or structural styles along the strike of the extensional system (e.g. [115–119]). Rift transfer faults are portrayed in the literature as pure strike-slip faults, when parallel to the extension direction, or as oblique-slip faults, with variable amount of dip displacement, when oblique to the extension direction [114, 115]. Both compressive (transpressional) and extensional (transtensional) structures may develop along transfer faults, depending on their angular relationship with the components of the extensional system [114]. Transfer faults usually connect major normal faults with similar or opposite polarities and their sense of slip is contrary to the apparent offset of the related normal faults [120]. Evolution of a transfer fault system may produce tectonic inversion, causing the migration of the subsiding depocentres parallel to the rift opening [116] (Figure 14B).

Along the Ionian coast of the Peloritani Mts, the combined activity of this complex fault system subdivided the coastal area into two main embayments (corresponding to the SW and NW sectors respectively) that subsided during two successive stages. The sedimentation of depositional cycle R2, filling the SW sector, occurred during the Early Pleistocene, while the NE sector was uplifted to form the northern margin of the palaeo-gulf (Figure 14C). No sedimentation occurred in the NE sector during this stage. Later, during the Middle Pleistocene, the SW sector was uplifted, and underwent deep erosion and cannibalization of pre-Pleistocene and R2 sediments. The recycled sediments were transported towards the subsiding NE sector

to form part of the younger depositional cycle R3 (Figure 14D) e.g. [89, 121].

The R2–R3 diachronism and the episodes of sediment recycling indicate the activity of a transfer fault system of local significance (as hypothesized in Figure 14B), whose existence is suggested by two main geological evidences: i) the main normal faults bounding the inner margin of the sedimentary succession are connected by transverse strike-slip minor faults, perpendicular to the shoreline, which do not propagate across the western crystalline basement (Figure 1); ii) especially for the SW sector, the pre-Pleistocene substrate is dissected by a number of shore-parallel normal faults which produce a series of tilted landward-dipping blocks. These two points confirm that these deformations may be related to the vertical displacement induced by a transfer fault active from Middle Pliocene onwards, as also argued by [45]. This system accommodated left-lateral strike-slip movement in the SW sector during the Lower Pleistocene (Figure 14C) and, later inverted its movement northwards, producing subsidence associated with right-lateral strike-slip in the NE sector during the Middle Pleistocene (Figure 14D).

This tectonic style characterized the opening of the Messina Strait, which reached its modern and definitive morphology at the end of the Pleistocene.

8. Insights on the opening of the Messina Strait

Facies associations influenced by tidally-driven currents are unusual for micro-tidal basins, such as the Mediterranean Sea, where tidal influence is often negligible along long-shore current- and/or wave-dominated coastal systems [82, 122]. However, similar tidally-influenced depositional settings were documented in the past from a number of late Cenozoic deposits in the central Mediterranean Sea, namely from the Pleistocene raised deposits occurring along the present-day Messina Strait margins [86].

In the study area, the Pleistocene hydrodynamic conditions were probably very similar to the present-day marine circulation: microtidal conditions are enhanced by the amplification of strong tidal currents in the local straits and coastal embayments located between the Tyrrhenian and Ionian seas [123]. An impressive example of this phenomenon is represented by the present-day Messina Strait, whose southward-sloping sublittoral to bathyal floor is dominated by descending tidal currents with velocities up to 1–3 m/s [71, 124]. All significant accumulations of Neogene tidal deposits in onshore Calabria and northern Sicily owe their origin to such specific settings, including the straits and embayments lo-

cated in central-southern Calabria and northern-eastern Sicily [106].

In the study succession, the tidally-influenced deposits are represented by cross-stratified sandstones that record amplification of tidal currents and are typically intercalated with gravity-driven deposits derived from the uplifted margins. Tidal control of sedimentation is not always present in the study succession. The Early Pleistocene deposits were dominated by wave-induced currents, characterizing the local coastal hydrodynamics. Sedimentation occurred under a steep coastal gradient and the deepest environments were probably under the influence of tidal currents flowing along the marginal part of the proto-Messina Strait.

Tidal signal is better recognized in the upper part of the younger succession R3, where biocalcarenic sediments are fully dominated by herringbone-type structures of ebb-flood tidal currents. This signal marks the opening of the Pleistocene Messina Strait, in which the amplification of the reverse currents from the two interlinked Tyrrhenian and Ionian basins prevailed over other hydrodynamic factors during Middle Pleistocene.

These data support the observations of [86] derived from study of analogous coastal successions cropping out along the Calabrian margin of the study area. These authors argued that the Messina Strait opening may have begun in the Middle Pleistocene, because only from this time did tidal currents begin to be amplified by a morpho-tectonic 'corridor', influencing the sedimentation of the coastal margins. This is in disagreement with other studies which have documented the individuation of this narrow linear basin starting from the Late Pliocene-Early Pleistocene e.g.: [4, 7, 50, 61, 123, 125, 126]. The onset of the daily inversion of strong tidal currents between the Tyrrhenian Sea and the Ionian Sea occurred most probably later, because no tide-influenced facies are documented from deposits that are older than the Middle Pleistocene.

9. Conclusions

This study represents the first effort to unravel depositional processes and sequence stratigraphy of mixed bioclastic/siliciclastic coastal deposits of the northern Ionian coast of Sicily (Southern Italy) during major relative sea level fluctuations of the Early-Middle Pleistocene, by means of integrated, high-resolution sedimentological and biostratigraphic approaches.

The investigated area is characterized by a biocalcarenic-dominated succession that can be divided into two main transgressive cycles, R2 and R3, that partially correlate with depositional sequences

previously detected across the northern (Tyrrhenian) coast of Sicily [22]. Cycle R2 was attributed to the MNN19d-MNN19e nannofossil biozones (1.5- 0.99 Ma) Early Pleistocene in age, whereas cycle R3 was confined to the Middle Pleistocene MNN19f zone (0.99-0.58 Ma).

The two cycles are formed by vertical successions of stratal units that can be subdivided into component facies associations. The sedimentary structures allow the interpretation of these facies associations as the response of the shoreface to offshore transition environments evolving to deeper conditions during marine transgressions.

Sedimentation occurred along a steep ramp-type shelf, variously dissected and compartmentalized by shore-parallel normal faults, creating accommodation space during sediment accumulation. This fault system (Ionian sector of the Siculo-Calabrian Rift Zone) produced a local transfer zone of strike-slip movement, which underwent a tectonic inversion during its evolution. This structural style, documented for extensional rift zones, caused dramatic subsidence of the sea floor during coastal wedge accretion, producing two diachronous, transgressive depositional cycles, that occur within two different sectors (SW and NE respectively). Subsidence progressively occurred northward along the coastal margin, producing alternating uplifted sectors. Concurrently the partial cannibalization of cycle R2 during the sedimentation of cycle R3 occurred.

The two cycles are interpreted as the transgressive counterparts of two separate successions, controlled by a virtually continuous tectonic subsidence. Cycle R2 also recorded the 41 ky glacial oscillations, as documented by the vertically stacked parasequences, whereas the deposition of cycle R3 was influenced by the 100 ky cycles resulting in a higher amplitude of the general transgression. Cycles R2 and R3 show retrograding-to slightly prograding systems tracts (TSTs and HSTs), recording two accretionary transgressions. The bulk of the TSTs are composed of retrogradational parasequence sets, marked at the base by discontinuous shell beds, characterized by deepening-upward trends in the vertically-stacked facies tracts and with the absence of any regressive trends.

Sediments forming the most distal facies of cycle R2 and the uppermost interval of cycle R3 became progressively influenced by tidal processes, suggesting the amplification of reverse tractional currents, instead of the 'normal' coastal hydrodynamics. These data suggest that the onset of the formation of the proto Messina Strait, that developed during the Late Pleistocene, is constrained to within the last 0.99-0.58 Ma, corresponding to the deposition of cycle R3.

Acknowledgements

This study has been funded by the Universities of Basilicata and Catania "Ateneo Grants (PRA)". An early version of the manuscript has benefited of the constructive comments of Prof. Francesco Massari (University of Padova, Italy) and Prof. Vincenzo Pascucci (University of Sassari, Italy). We are grateful to Prof. Riccardo Caputo (University of Ferrara, Italy) for his useful suggestions and comments concerning the tectonic model. The authors wish to thank Dr. Jiri Laurin (Geophysical Institute, Prague, Czech Republic), Dr. Paola Ronchi (Eni S.p.A. E&P Division, San Donato Milanese, Italy) and Prof. Gabriele Carannante (University of Napoli, Italy), whose constructive contributions highly improved the final version of the paper.

References

- [1] Barrier P., Évolution paléogéographique du détroit de Messine au Pliocène et au Pléistocène, *Giornale di Geologia*, 1986, 3, 48, 7-24
- [2] Barrier P., Stratigraphie des dépôts pliocènes et quaternaires du Déroit de Messine, *Documents et Travaux d'Institut géologique Albert de Lapparent (IGAL)*, 1987, 11, 59-81
- [3] Bonfiglio L., Nuovi elementi faunistici e stratigrafici del Pleistocene superiore dei Nebrodi (Sicilia nord-orientale), *Riv. Ital. Paleontol. S.*, 1987, 93, 145-164
- [4] Barrier P., Di Geronimo I., Montenat C., Le Déroit de Messine (Italie), évolution tectono-sédimentaire récente (Pliocène et Quaternaire) et environnement actuel, *Documents et Travaux d'Institut géologique Albert de Lapparent (IGAL) (Paris)*, 1987
- [5] Barrier P., Di Geronimo I., Montenat C., Roux M., Zibrowius H., Présence de faunes bathyales atlantiques dans le Pliocène et le Pléistocène de la Méditerranée (Détroit de Messine, Italie), *B. Soc. Geol. Fr.*, 1989, 8, 87-796
- [6] Fois E., La successione neogenica di Capo Milazzo (Sicilia Nord-Orientale), *Riv. Ital. Paleontol. S.*, 1990, 95, 397-440
- [7] Montenat C., Barrier P., Ott d'Estevou P., Some aspects of the recent tectonics in the Strait of Messina, Italy, *Tectonophysics*, 1991, 194, 203-215
- [8] Di Geronimo I., d'Atri A., La Perna R., Rosso A., Sanfilippo R., Violanti D., The Pleistocene bathyal section of Archi (Southern Italy), *Bollettino della Società Paleontologica Italiana*, 1997, 36, 189-212
- [9] Di Geronimo I., Messina C., Rosso A., Sanfilippo R., Sciuto F., Vertino A., Enhanced biodiversity in the deep: Early Pleistocene coral communities from southern Italy, In: *Freiwald A., Roberts J. M. (Eds.), Cold-water Corals and Ecosystems*, Springer-Verlag Berlin, 2006
- [10] Di Stefano A., Lentini R., Ricostruzione stratigrafica e significato paleotettonico dei depositi Plio-Pleistocenici del margine tirrenico tra Villafranca Tirrena e Faro (Sicilia nord-orientale), *Studi Geologici Camerti*, 1995, 2, 219-237
- [11] Bellotti P., Evangelista S., Tortora P., Valeri P., Caratteri sedimentologici e stratigrafici dei sedimenti Plio-Pleistocenici affioranti lungo la costa tra Tor Caldara e Anzio (Lazio centrale), *Bollettino della Società Paleontologica Italiana*, 1997, 116, 79-94
- [12] Butler R.W.H., Grasso M., Gardiner W., Sedgely D., Depositional patterns and their tectonic controls within the Plio-Quaternary carbonate sands and muds of onshore and offshore SE Sicily (Italy), *Mar. Petrol. Geol.*, 1998, 14, 879-892
- [13] Catalano R., Di Stefano E., Infuso S., Sulli A., Vail P.R., Vitale F.P., Sequence and systems tracts calibrated by high-resolution biostratigraphy: the central Mediterranean Plio-Pleistocene record, In: *De Graciansky P.C., Hardenbol J., Jacquin T., Vail P.R. (Eds.), Mesozoic-Cenozoic sequence stratigraphy of European Basins. Soc. Econom., Society of Economy, Paleontology, Mineralogy, Spec. publ.*, 1998, 60, 157-179
- [14] Hansen K.S., Development of a prograding carbonate wedge during sea level fall: Lower Pleistocene of Rhodes, Greece, *Sedimentology*, 1999, 46, 559-576
- [15] Massari F., Rio D., Sgavetti M., Interplay between tectonics and glacio-eustasy: Pleistocene succession of the Crotona basin, Calabria, *Geol. Soc. Am. Bull.*, 2002, 114, 1183-1209
- [16] Pedley M., Grasso M., Lithofacies modelling and sequence stratigraphy in microtidal cool-water carbonates: a case study from the Pleistocene of Sicily, Italy, *Sedimentology*, 2002, 49, 533-553
- [17] Capozzi R., Picotti V., Pliocene sequence stratigraphy, climatic trends and sapropel formation in the Northern Apennines (Italy), *Palaeogeogr. Palaeoclimatol.*, 2003, 190, 349-371
- [18] Roveri M., Taviani M., Calcarene and sapropel deposition in the Mediterranean Pliocene: shallow- and deepwater record of astronomically driven climatic events, *Terra Nova*, 2003, 15, 279-286
- [19] Martín J.M., Braga J.C., Aguirre J., Betzler, C., Contrasting models of temperate carbonate sedimentation in a small Mediterranean embayment: the

- Pliocene Carboneras Basin, SE Spain, *J. Geol. Soc. London*, 2004, 161, 387-399
- [20] Titschack J., Bromley R.G., Freiwald A., Plio-Pleistocene cliff-bound, wedge-shaped, warm-temperate carbonate deposits from Rhodes (Greece): sedimentology and facies, *Sediment. Geol.*, 2005, 180, 29-56
- [21] Massari F., Chiocci F.L., Biocalcarene and mixed cool-water prograding bodies of the Mediterranean Pliocene and Pleistocene: architecture, depositional setting and forcing factors, In: Pedley H.M., Carannante G. (Eds.), *Cool-Water Carbonates: Depositional Systems and Palaeoenvironmental Controls*, *J. Geol. Soc. London, Spec. Publ.*, 2006, 255, 95-120
- [22] Di Stefano A., Longhitano S.G., Smedile A., Sedimentation and tectonics in a steep shallow-marine depositional system: stratigraphic arrangement of the Plio-Pleistocene Rometta succession, NE Sicily (Italy), *Geol. Carpath.*, 2007, 58, 71-87
- [23] Critelli S., Le Pera E., Galluzzo F., Milli S., Moscatelli M., Perrotta S. et al., Interpreting siliciclastic-carbonate detrital modes in foreland basin systems: an example from Upper Miocene arenites of the central Apennines, Italy, In: Johnsson M., Arribas J., Critelli S. (Eds.), *Sedimentary Provenance and Petrogenesis: Perspectives from Petrography and Geochemistry*, *Geological Society of America, Spec. Publ.*, 2007, 420, 107-133
- [24] Messina C., Rosso A., Sciuto F., Di Geronimo I., Nemeč W., Di Dio T. et al., Anatomy of a transgressive systems tract revealed by integrated sedimentological and palaeoecological study: the Barcellona P.G. Basin, northeastern Sicily, Italy, In: Nichols G., Paola C., Williams E.A. (Eds.), *Sedimentary Processes, Environments and Basins - A Tribute to Peter Friend*, *International Association of Sedimentologists, Spec. Publ.*, 2007, 367-398
- [25] Massari F., Sgavetti M., Rio D., D'Alessandro A., Prosser G., Composite sedimentary record of falling stages of Pleistocene glacio-eustatic cycles in a shelf setting (Crotone basin, south Italy), *Sediment. Geol.*, 1999, 127, 85-110
- [26] Plint A.G., Norris B., Anatomy of a ramp margin sequence: facies successions, paleogeography and sediment dispersal patterns in the Muskiki and Marshy bank formation, Alberta Foreland Basin, *B. Can. Petrol. Geol.*, 1991, 39, 18-42
- [27] Read J.F., Phanerozoic carbonate ramps from greenhouse, transitional, and ice-house worlds: clues from field and modeling studies, In: Wright V.P., Burchette T.P. (Eds.), *Carbonate Ramps*, *J. Geol. Soc. London, Spec. Publ.*, 1998, 149, 107-136
- [28] Mount J.F., Mixing of siliciclastic and carbonate sediments in shallow shelf environments, *Geology*, 1984, 12, 432-435
- [29] Zuffa G.G., Hybrid arenites: their composition and classification, *J. Sediment. Res.*, 1980, 50, 21-29
- [30] Lees A., Possible influences of salinity and temperature on modern shelf carbonate sedimentation, *Mar. Geol.*, 1975, 19, 159-198
- [31] Carannante G., Esteban M., Milliman J.D., Simone L., Carbonate lithofacies as paleolatitude indicators: problems and limitations, *Sediment. Geol.*, 1988, 60, 333-346
- [32] Gargano C., Carta Geologica di Messina e del settore nord-orientale dei Monti Peloritani, scale 1:25.000, S.El.Ca., Florence, 1994
- [33] Lentini F., Catalano S., Carbone S., Geological map of Messina province (NE Sicily), scale 1:50.000, Società di Elaborazione Cartografica, Florence, 2000
- [34] Finetti I.R., Lentini F., Carbone S., Del Ben A., Di Stefano A., Forlin E. et al., Geological Outline of Sicily and Lithospheric Tectono-Dynamics of its Tyrrhenian Margin from New CROP Seismic Data, In: Finetti I.R. (Ed.), *CROP Project: Deep Seismic Exploration of the Central Mediterranean and Italy*, Elsevier, 2005
- [35] Amodio Morelli L., Bonardi G., Colonna V., Dietrich D., Giunta G., Ippolito F. et al., L'Arco Calabro-Peloritano nell'orogene Appenninico-Maghrebide, *Memorie della Società Geologica Italiana*, 1976, 17, 1-60
- [36] Ghisetti F., Vezzani L., The recent deformation mechanism of the Calabrian Arc, *Earth and Environmental Sciences*, 1982, 3, 2, 197-206
- [37] Dewey J.F., Helman M.L., Turco E., Hutton D.H.W., Knott S.D., Kinematics of the Western Mediterranean, In: Coward M.P., Dietrich D., Park R.G. (Eds.) *Alpine Tectonics*, *Geological Society of America, Spec. Publ.*, 1989, 45, 265-284
- [38] Lentini F., Carbone S., Catalano S., Main structural domains of the central Mediterranean region and their tectonic evolution, *Bollettino di Geofisica Teorica ed Applicata*, 1994, 36, 141-144, 103-125
- [39] Finetti I.R., Lentini F., Carbone S., Catalano S., Del Ben A., Il sistema Appennino Meridionale-Arco Calabro-Sicilia nel Mediterraneo centrale: studio geologico-geofisico, *Bollettino della Società Geologica Italiana*, 1996, 115, 529-559
- [40] Malinverno A., Ryan W.B.F., Extension in the Tyrrhenian Sea and shortening in the Apennines as a result of arc migration driven by sinking of the lithosphere, *Tectonics*, 1986, 5, 227-245
- [41] Royden L., Patacca E., Scandone P., Segmentation

- and configuration of subducted lithosphere in Italy: an important control on thrust-belt and foredeep-basin evolution, *Geology*, 1987, 15, 714-717
- [42] Doglioni C., A proposal of kinematic modeling for W-dipping subductions. Possible applications to the Tyrrhenian-Apennines system, *Terra Nova*, 1991, 3, 423-434
- [43] Critelli S., The interplay of lithospheric flexure and thrust accommodation in forming stratigraphic sequences in the southern Apennines foreland basin system, Italy, *Rendiconti dell'Accademia dei Lincei*, 1999, 9, 257-326
- [44] Lentini F., Carbone S., Catalano S., Di Stefano A., Gargano C., Romeo M. et al., Sedimentary evolution of basins in mobile belts: examples from tertiary terrigenous sequences of the Peloritani Mts (NE Sicily), *Terra Nova*, 1995, 7, 161-170
- [45] Monaco C., Tortorici L., Nicolich R., Cernobori L., Costa M., From collisional to rifted basins: an example from the southern Calabrian Arc (Italy), *Tectonophysics*, 1996, 266, 233-249
- [46] Guarnieri P., Di Stefano A., Carbone S., Lentini F., Del Ben A., A multidisciplinary approach to the reconstruction of the Quaternary evolution of the Messina Strait (including: Geological Map of the Messina Strait area, scale 1:25.000), In: Pasquarè G., Venturini C. (Eds.) *Mapping Geology of Italy*, 2005, (APAT) Agenzia per la Protezione dell'Ambiente e per i Servizi Tecnici, 44-50
- [47] Seguenza G., Studi stratigrafici sulla formazione pliocenica dell'Italia meridionale, *Bollettino e Rendiconti della Commissione di Geologia*, 1873-1877, I, 4-7
- [48] Ogniben L., Explicative notes of the geological scheme of NE Sicily, *Rivista Mineraria Siciliana*, 1960, 64-65, 183-212
- [49] Bonfiglio L., Berdar A., Elefanti pleistocenici del litorale dello Stretto di Messina, revisione e nuove osservazioni, *Quaternaria*, 1969, 11, 255-261
- [50] Zeliglis A., The geometry of fan-deltas and related turbidites in narrow linear basins, *Geol. J.*, 2003, 38, 31-46
- [51] Ghisetti F., Recent deformations and the seismogenic source in the Messina Strait (Southern Italy), *Tectonophysics*, 1984, 109, 191-208
- [52] Ghisetti F., Fault parameters in the Messina Strait (Southern Italy) and relations with the seismogenic source, *Tectonophysics*, 1992, 210, 117-133
- [53] Monaco C., Tortorici L., Active faulting in the Calabrian Arc and Eastern Sicily, *J. Geodyn.*, 2000, 29, 407-424
- [54] Catalano S., De Guidi G., Monaco C., Tortorici G., Tortorici L., Active faulting and seismicity along the Siculo-Calabrian Rift Zone (Southern Italy), *Tectonophysics*, 2008, 453, 177-192
- [55] Tortorici L., Monaco C., Tansi C., Cocina O., Recent and active tectonics in the Calabrian Arc (southern Italy), *Tectonophysics*, 1995, 243, 37-49
- [56] Lentini F., Carbone S., Catalano S., Grasso M., Elementi per la ricostruzione del quadro strutturale della Sicilia orientale, *Memorie della Società Geologica Italiana*, 1996, 51, 179-195
- [57] Jacques E., Monaco C., Tapponnier P., Tortorici L., Winter T., Faulting and earthquake triggering during the 1783 Calabria seismic sequence, *Geophys. J. Int.*, 2001, 499-516
- [58] Galli P., Bosi V., Paleoseismology along the Citanova fault: implications for seismotectonics and earthquake recurrence in Calabria (Southern Italy), *J. Geophys. Res.*, 2002, 107, B3, 1-18
- [59] Catalano S., De Guidi G., Late Quaternary uplift of northeastern Sicily: relation with the active normal faulting deformation, *J. Geodyn.*, 2003, 36, 445-467
- [60] Monaco C., Tortorici L., Tettonica estensionale quaternaria nell'Arco Calabro e in Sicilia orientale, *Studi Geologici Camerti*, 1995, 2, 351-362
- [61] Ghisetti F., Upper Pliocene-Pleistocene uplift rates as indicators of neotectonic pattern: an example from Southern Calabria (Italy), *Z. Geomorphol.*, 1981, 40, 93-118
- [62] Dumas B., Gueremy P., Lhenaff R., Raffy J., Le soulèvement quaternaire de la Calabrie méridionale, *Rev. Geol. Dyn. Geogr.*, 1982, 23, 27-40
- [63] Dumas B., Gueremy P., Lhenaff R., Raffy J., Rates of uplift as shown by raised Quaternary shorelines in Southern Calabria (Italy), *Z. Geomorphol.*, NF suppl. Bd., 1987, 63, 119-132
- [64] Westaway R., Quaternary uplift of Southern Italy, *J. Geophys. Res.*, 1993, 98, 21741-21772
- [65] De Guidi G., Catalano S., Monaco C., Tortorici L., Di Stefano A., Long-term effects of late Quaternary normal faulting in southern Calabria and Eastern Sicily, *Studi Geologici Camerti, nuova serie*, 2002, 1, 79-93
- [66] Antonioli F., Ferranti L., Lambeck K., Kershaw S., Verrubbi V., Dai Pra G., Late Pleistocene to Holocene record of changing uplift rates in southern Calabria and northeastern Sicily (southern Italy, Central Mediterranean Sea), *Tectonophysics*, 2006, 422, 23-40
- [67] Valensise G., Pantosti D., A 125 kyr-long geological record of seismic source repeatability: the M.S.s (southern Italy) and the 1908 earthquake (MS 7 1/2), *Terra Nova*, 1992, 4, 472-483

- [68] Catalano S., De Guidi G., Monaco C., Tortorici G., Tortorici L., Long-term behaviour of the late Quaternary normal faults in the Straits of Messina area (Calabrian Arc): structural and morphological constraints, *Quatern. Int.*, 2003, 101-102, 81-91
- [69] Ryan W.B.F., Heezen B.C., Ionian Sea submarine canyons and the 1908 Messina turbidity current, *Geol. Soc. Am. Bull.*, 1965, 76, 915-934
- [70] Selli R., Colantoni P., Fabbri A., Rossi S., Borsetti A.M., Galignani P., Marine Geological Investigations on the Messina Strait and its approaches, *Giornale di Geologia*, 1978, 42, 1-70
- [71] Santoro V.C., Amore E., Cavallaro L., Cozzo G., Foti E., Sand waves in the Messina Strait, Italy, *J. Coastal Res.*, 2002, 36, 640-653
- [72] Fornaciari E., Rio D., Latest Oligocene to Early Middle Miocene quantitative calcareous nannofossils biostratigraphy in the Mediterranean region, *Micropaleontology*, 1996, 42, 1-36
- [73] Rio D., Raffi I., Villa G., Pliocene-Pleistocene nannofossil distribution patterns in the Western Mediterranean, In: Kastens K.A., Mascle J., et al. (Eds.), *Proceedings of the Ocean Drilling Program Scientific Report*, 1990, 107, 513-533
- [74] Cita M.B., Planktic foraminiferal biozonation of the mediterranean Pliocene deep sea record: a revision, *Rivista Italiana di Paleontologia e Stratigrafia*, 1975, 81, 527-544
- [75] Sprovieri R., Di Stefano E., Howell M., Sakamoto T., Di Stefano A., Marino M., Integrated calcareous plankton biostratigraphy and cyclostratigraphy at site 964, In: Robertson A.H.F., Emeis K.C., Richter C., et al. (Eds.), *Proceedings of the Ocean Drilling Program Scientific Report*, 1998, 160, 155-165
- [76] Van Couvering J.A., Preface: the new Pleistocene, In: Van Couvering J.A. (Ed.), *The Pleistocene boundary and the beginning of the Quaternary*, Cambridge University Press, 1997
- [77] Richmond G.M., The INQUA-approved provisional Lower-Middle Pleistocene boundary, In: Turner C. (Ed.), *The Early Middle Pleistocene in Europe*, Balkema Rotterdam, 1996
- [78] Gradstein F., Ogg J., Smith A., *A Geologic Time Scale 200*, Cambridge University Press, Cambridge, 2004
- [79] Einsele G., Ricken W., Seilacher A., *Cycles and events in stratigraphy*, Springer-Verlag Berlin, Heidelberg, 1991
- [80] Zecchin M., The architectural variability of small-scale cycles in shelf and ramp clastic systems: the controlling factors, *Earth-Sci. Rev.*, 2007, 84, 21-55
- [81] Titschack J., Vertino A., Pino P., Rosso A., Pliocene cold-water coral deposits at la Montagna (Messina, Sicily) - submarine dune or cold-water coral mound?, SDGG, 26th Regional Meeting of IAS, Abstract Volume, 2008
- [82] Orton G.J., Reading H.G., Variability of deltaic processes in terms of sediment supply, with particular emphasis on grain size, *Sedimentology*, 1993, 40, 475-512
- [83] Wright L.D., Chappell J., Thom B.G., Bradshaw M.P., Cowell P., Morphodynamics of reflective and dissipative beach and inshore systems, southeastern Australia, *Mar. Geol.*, 1979, 32, 105-140
- [84] Vertino A., Esacoralli plio-pleistocenici e attuali del Mediterraneo (sistemática, biostratinomia, paleoecologia), *PaleoItalia*, 2004, 10, 22-25
- [85] Álvarez-Pérez G., Busquets P., De Mol B., Sandoval Nicolás G., Canals M., Casamor J.L., Deep-water corals occurrences in the Strait of Gibraltar, In: Freiwald A., Roberts J.M. (Eds.) *Cold-water corals and ecosystems*, Springer-Verlag Berlin, Heidelberg, 2006
- [86] Mercier D., Barrier P., Beaudoin B., Didier S., Montenat J.L., Salinas Zuniga E., Les facteurs hydrodynamiques dans la sédimentation plio-quaternaire du Déroit de Messine, *Documents et Travaux de l'Institut Géologique A. De Lapparent*, Paris, 1987, 11, 171-183
- [87] Lees A., Buller A.T., Modern temperate water and warm water shelf carbonate sediments contrasted, *Mar. Geol.*, 1972, 13, 67-73
- [88] Nelson C.S., Keane S.L., Head P.S., Non-tropical carbonate deposits on the modern New Zealand shelf, *Sediment. Geol.*, 1988, 60, 71-94
- [89] Critelli S., Arribas J., Le Pera E., Tortosa A., Marsaglia K.M., Latter K.K., The recycled orogenic sand provenance from an uplifted thrust belt, Betic Cordillera, Southern Spain, *J. Sediment. Res.*, 2003, 73, 72-91
- [90] Morales J.A., Borrego J., Jiménez I., Monterde J., Gil N., Morphostratigraphy of an ebb-tidal delta system associated with a large spit in the Piedras Estuary mouth (Huelva Coast, Southwestern Spain), *Mar. Geol.*, 2001, 172, 225-241
- [91] Chiocci F.L., Orlando L., Lowstand terraces on Tyrrhenian Sea steep continental slopes, *Mar. Geol.*, 1996, 134, 127-143
- [92] Pomar L., Tropeano M., The Calcarenite di Gravina Formation in Matera (southern Italy): new insights for coarsegrained, large-scale, crossbedded bodies encased in offshore deposits, *A. A. P. G. Bull.*, 2001, 85, 661-689
- [93] Chiocci F.L., D'Angelo S., Romagnoli C., Atlante

- dei Terrazzi Deposizionali Sommersi lungo le coste italiane, *Memorie Descrittive della Carta Geologica d'Italia*, 2004, 58, 1-194
- [94] Martín J.M., Braga J.C., Aguirre J., Betzler C., Contrasting models of temperate carbonate sedimentation in a small Mediterranean embayment: the Pliocene Carboneras Basin, SE Spain, *J. Geol. Soc. London*, 2004, 161, 387-399
- [95] Galloway W.E., Genetic stratigraphic sequences in basin analysis, I. Architecture and genesis of flooding-surface bounded depositional units, *A. A. P. G. Bull.*, 1989, 73, 125-142
- [96] Catuneanu O., Willis A.J., Miall A.D., Temporal significance of sequence boundaries, *Sediment. Geol.*, 1998, 121, 157-178
- [97] Helland-Hansen W., Gjelberg J.G., Conceptual basis and variability in sequence stratigraphy: a different perspective, *Sediment. Geol.*, 1994, 92, 31-52
- [98] Cattaneo A., Steel R.J., Transgressive deposits: a review of their variability, *Earth-Sci. Rev.*, 2003, 62, 187-228
- [99] Goldhammer R.K., Dunn P.A., Hardie L.A., Depositional cycles, composite sea level changes, cycle stacking patterns and the hierarchy of stratigraphic forcing – examples from Alpine Triassic platform carbonates, *Geol. Soc. Am. Bull.*, 1990, 102, 535-562
- [100] Soreghan G.S., Dickinson W.R., Generic types of stratigraphic cycles controlled by eustasy, *Geology*, 1994, 22, 759-761
- [101] Kidwell S.M., Condensed deposits in siliciclastic sequences: expected and observed features, In: Einsele G., Ricken W., Seilacher A. (Eds.), *Cycles and Events in Stratigraphy*, Springer-Verlag Berlin, Heidelberg, 1991
- [102] Abbott S.T., Carter R.M., The sequence architecture of mid-Pleistocene (c. 1.1-0.4 Ma) cyclothems from New Zealand: facies development during a period of orbital control on sea-level cyclicity, *International Association of Sedimentologists, Spec. Publ.*, 1994, 19, 367-394
- [103] Naish T., Kamp P.J.J., Sequence stratigraphy of sixth-order (41 k.y.) Pliocene-Pleistocene cyclothems, Wanganui basin, New Zealand: a case for the regressive systems tract, *Geol. Soc. Am. Bull.*, 1997, 109, 8, 978-999
- [104] Van Wagoner J.C., Posamentier H.W., Mitchum R.M., Vail, P.R., Loutit T.S., Hardenbol J., An overview of the fundamentals of sequence stratigraphy and key definitions, In: Wilgus C.K., Hastings B.S., Kendall C.G., Posamentier H.W., Ross C.A., Van Wagoner J.C. (Eds.), *Sea-Level changes: an integrated approach*, Society for Economy, Paleontology and Mineralogy, Special Publication, 1988, 42, 39-45
- [105] Van Wagoner J.C., Mitchum R.M., Campion K.M., Rahmanian V.D., Siliciclastic sequence stratigraphy in well logs, cores and outcrops, *American Association of Petroleum Geologists Methods in Exploration* 1990, 7, 1-55
- [106] Longhitano S.G., Nemeč W., Statistical analysis of bed-thickness variation in a Tortonian succession of biocalcarenitic tidal dunes, Amantea Basin, Calabria, southern Italy, *Sediment. Geol.*, 2005, 179, 3-4, 195-224
- [107] Galloway W.E., Depositional processes, regime variables, and development of siliciclastic stratigraphic sequences, In: Gradstein F.M., Sandvik K.O., Milton N.J. (eds), *Sequence Stratigraphy-Concepts and Application*, Norwegian Petroleum Society, Spec. Publ., 1998, 8, 117-140
- [108] Lisiecki L.E., Raymo M.E., A Pliocene-Pleistocene stack of 57 globally distributed benthic 18O records, *Paleoceanography*, 2005, 20, PA1003
- [109] Lisiecki L.E., Raymo M.E., Plio-Pleistocene climate evolution: trends and transitions in glacial cycle dynamics, *Quaternary Sci. Rev.*, 2007, 26, 56-69
- [110] Bintanja R., van de Wal R.S.W., North-American ice-sheet dynamics and the onset of 100,000-year glacial cycles, *Nature*, 2008, 454, 869-872
- [111] Clark P.U., Pollard D., The origin of the middle Pleistocene transition by ice sheet erosion of regolith, *Paleoceanography*, 1998, 13, 1-9
- [112] Ziperman E., Gildor H., On the mid-Pleistocene transition to 100-kyr glacial cycles and the asymmetry between glaciation and deglaciation times, *Paleoceanography*, 2003, 18, 1001
- [113] Jervey M.T., Quantitative geological modeling of siliciclastic rock sequences and their seismic expression. In: Wilgus C.K., Hastings B.S., Posamentier H.W., Van Wagoner J.C., Ross C.A., Kendall C.G. (Eds.), *Sea-level Changes – an Integrated Approach*, Society for Economy, Paleontology and Mineralogy, Special Publication, 1988, 42, 47-69
- [114] Gibbs A.D., Structural evolution of extensional basin margins, *J. Geol. Soc. London*, 1984, 141, 609-620
- [115] Lister G.S., Etheridge M.A., Symonds P.A., Detachment faulting and the evolution of the passive continental margins, *Geology*, 1986, 14, 246-250
- [116] Milani E.J., Davison I., Basement control, and transfer tectonics in the Recôncavo-Tucano-Jatobá rift, Northeast Brazil, *Tectonophysics*, 1988, 154, 41-70
- [117] Bosworth W., A high-strain rift model for the southern Gulf of Suez (Egypt), In: Lambiase J.J. (ed.), *Hydrocarbon Habitats in Rift Basins*, *J. Geol. Soc. London, Special Publication*, 1995, 80, 75-102

- [118] Salah M.G., Alsharhan A.S., Structural influence on hydrocarbon entrapment in the Northwestern North Sea, Egypt, *A. A. P. G. Bull.*, 1996, 80, 101-118
- [119] McClay K., Khalil S., Extensional hard linkages, eastern Gulf of Suez, Egypt, *Geology*, 1998, 26, 563-566
- [120] Gibbs A.D., Linked fault families in basin formation, *J. Struct. Geol.*, 1990, 12, 795-803
- [121] Critelli S., Rumelhart P.E., Ingersoll R.V., Petrofacies and provenance of the Puente Formation (middle to upper Miocene), Los Angeles Basin, Southern California; implications for rapid uplift and accumulation rates, *J. Sediment. Res.*, 1995, 65, 656-667
- [122] Hampson G.J., Storms J.E.A., Geomorphological and sequence stratigraphic variability in wave-dominated, shoreface-shelf parasequences, *Sedimentology*, 2003, 50, 667-701
- [123] Colella A., D'Alessandro A., Sand waves, Echinocardium traces and their bathyal depositional setting (Monte Torre Palaeostrait, Plio-Pleistocene, southern Italy), *Sedimentology*, 1988, 35, 219-237
- [124] Montenat C., Barrier P., Di Geronimo I., The Strait of Messina, past and present: a review, *Documents et Travaux d'Institut Geologique A. De Lapparent*, Paris, 1987, 11, 7-13
- [125] Bousquet J.C., Carveni P., Lanzafame G., Philip H., Tortorici L., La distension pleistocene sur le bord oriental du détroit de Messine: analogies entre les résultats microtectoniques et le mécanisme au foyer du séisme de 1908, *B. Soc. Geol. Fr.*, 1980, 12, 327-336
- [126] Sauret B., Contribution a l'étude néotectonique du Déroit de Messine (Italie, secteur sud de Reggio de Calabria), PhD Thesis, University of Paris VII, 1980, France